THE JOURNAL OF BIOLOGICAL CHEMISTRY VOL. 288, NO. 19, pp. 13278–13294, May 10, 2013

Regulation of the Bone-restricted IFITM-like (*Bril*) Gene Transcription by Sp and Gli Family Members and CpG Methylation*[S]

Received for publication, January 29, 2013, and in revised form, March 14, 2013 Published, JBC Papers in Press, March 24, 2013, DOI 10.1074/jbc.M113.457010

Bahar Kasaai[‡], Marie-Hélène Gaumond[‡], and Pierre Moffatt[‡§1]

From the [‡]Shriners Hospital for Children, Montreal, Quebec H3G 1A6, Canada and the [§]Department of Human Genetics, McGill University, Montreal, Quebec H3A 1B1, Canada

Background: BRIL is a bone-specific membrane protein that is involved in osteogenesis imperfecta type V.
Results: *Bril* transcription is activated by Sp1, Sp3, OSX, and GLI2 and by CpG demethylation.
Conclusion: Regulation of *Bril* involves trans-acting factors integrating at conserved promoter elements and epigenetic modifications.
Significance: Identification of the mechanisms governing *Bril* transcription is important to understand its role in skeletal biology.

***Bril* encodes a small membrane protein present in osteoblasts. In humans, a single recurrent mutation in the 5′-UTR of *BRIL* causes osteogenesis imperfecta type V. The exact function of BRIL and the mechanism by which it contributes to disease are still unknown. The goal of the current study was to characterize the mechanisms governing *Bril* transcription in humans, rats, and mice. In the three species, as detected by luciferase reporter assays in UMR106 cells, we found that most of the base-line regulatory activity was localized within ~250 bp upstream of the coding ATG. Co-transfection experiments indicated that Sp1 and Sp3 were potent inducers of the promoter activity, through the binding of several GC-rich boxes. Osterix was a weak activator but acted cooperatively with Sp1 and GLI2 to synergistically induce the *BRIL* promoter. GLI2, a mediator of hedgehog signaling pathway, was also a potent activator of *BRIL* through a single GLI binding site. Correspondingly, agonists of the hedgehog pathway (purmorphamine and Indian hedgehog) in MC3T3 osteoblasts led to increased BRIL levels. The *BRIL* promoter activity was also found to be negatively modulated through two different mechanisms. First, the ZFP354C zinc finger protein repressed basal and Sp1-induced activity. Second, CpG methylation of the promoter region correlated with an inactive state and prevented Sp1 activation. The data provide the very first analyses of the cis- and trans-acting factors regulating *Bril* transcription. They revealed key roles for the Sp members and GLI2 that possibly cooperate to activate *Bril* when the promoter becomes demethylated.**

Bril (bone-restricted Ifitm-like, or *Ifitm5*) was discovered as part of a high throughput screen for cDNAs encoding secreted and membrane proteins in osteoblastic cells (1). BRIL is part of an evolutionarily conserved family of so-called small interferon-inducible transmembrane (IFITM) proteins (2), for which there are at least four closely related members in humans (IFITM1, -2, -3, and -10) (3, 4). The mouse has two other members (IFITM6 and -7). The term "dispanin" has been coined recently to encompass IFITMs into an even larger family of proteins that have two transmembrane passages (4).

The classification of BRIL, however, as part of this family of IFITMs is based on general rather than functional considerations. *BRIL*, *IFITM1*, *IFITM2*, and *IFITM3* are all clustered within 25 kb on chromosome 11 (in humans); they all possess a similar gene architecture comprising two small coding exons separated by a short intron and a potentially similar predicted protein topology, having two transmembrane domains. Immunolocalization studies using tagged BRIL (5) and IFITM3 (6, 7) suggested that they have both their N and C termini extruding out into the extracellular space, although this predicted model has been challenged recently at least for IFITM3 (8, 9). Furthermore, other members like IFITM3 seem to localize preferentially into the endosome compartment (8, 9), whereas BRIL localizes mostly to plasma membranes (5). BRIL presents some other features that make it a distinctive member. For instance, unlike other IFITM members, which are highly inducible by type I interferons due to the presence of interferon regulatory elements in their promoter region (10), *Bril* transcription is not responsive to interferons (11). More importantly, we have shown that expression of *Bril* is mostly restricted to osteoblasts (5), whereas other *Ifitm* genes are ubiquitous. Expression of *Bril* was confirmed to be enriched in bone tissues in humans (12) and in the tammar wallaby (3) and increased under culture conditions favoring osteogenic differentiation (13).

At the functional level, our group was the first to suggest that BRIL is a positive modulator of mineralization via overexpression and knockdown studies in cultured osteoblasts (5). The molecular mechanisms of BRIL action in osteoblasts, however, have yet to be uncovered. Whether BRIL contributes directly to mineralization by interacting with its extracellular environment/matrix and/or indirectly in association with other mem-

* This work was supported in part by a grant from the Shriners of North America and by a Recruitment Aid program from the Network of Oral and Bone Health Research of the Fonds de Recherche du Quebec en Sante.
[S] This article contains supplemental Table 1 and Figs. 1–3.
[1] To whom correspondence should be addressed: Shriners Hospital for Children, 1529 Cedar Ave., Montreal, Quebec H3G 1A6, Canada. Tel.: 514-282-7161; Fax: 514-842-5581; E-mail: pmoffatt@shriners.mcgill.ca.

brane and intracellular mediators is still unknown. An interesting hypothesis put forward is that BRIL could be involved in calcium binding through its conserved aspartate-rich C-terminal end (2), a domain reminiscent of EF-hand structure (14). Also, BRIL was found to interact with other transmembrane proteins, such as FK506-binding protein 11, an association that appears to modulate complex assembly with the tetraspanin proteins CD9 and CD81 (15). It remains to be determined whether these interactions occur *in vivo* and contribute to BRIL function.

Studies exploring the function of *Bril* by genetic approaches in mice have yielded equivocal evidence. A knock-out mouse model for *Bril* was reported to have breeding problems and displayed only a subtle and transient reduction in bone length and structure in embryos and neonatal mice, without any evidence for changes in bone morphometric parameters (16). In contrast, our own *Bril* knock-out/LacZ knock-in mouse did not present any developmental and reproductive problems and did not show any appreciable mineralization defects in their skeletons.[2] In addition, genetic ablation in mice of either *Ifitm3* alone or the entire locus comprising *Ifitm1*, *-2*, and *-3* and *Bril* did not present any apparent physiological phenotype under normal conditions (17). What has emerged recently is the prominent role of IFITM1, -2, and -3 in inhibition in cell entry and infection by various viruses (6, 18–23), a function dependent on palmitoylation of conserved cysteine residues (7, 9).

Clearly, the information gained from existing mouse models has not allowed one to conclusively infer a function for BRIL in the skeleton (15, 17), despite marked effects observed *in vitro* on osteoblast activity (5). Two independent studies, however, found that a mutation in the 5′-UTR region of the *BRIL* gene is the cause of osteogenesis imperfecta (OI)[3] type V (12, 25). OI type V is inherited in an autosomal dominant fashion, and patients with OI type V display distinct clinical features not usually observed in any other OI type, such as hyperplastic callus formation and interosseous membrane ossification (26). The mutation found (c.−14C→T) creates a novel in frame ATG upstream of the natural coding start of BRIL, resulting in an extension of 5 residues (MALEP) at its N terminus. Our group has now confirmed that this single recurrent mutation is present in 42 individuals with type V OI (27). It has been proposed that the N terminus extension of the mutant BRIL is a gain of detrimental function, but the underlying molecular mechanism is still elusive.

Nothing is presently known about the regulation of the *Bril* gene regulation. The aim of the current study was to characterize the mechanisms governing *Bril* transcription. More specifically, we mapped the promoter cis-acting regulatory elements essential for the osteoblast-specific expression of *Bril* in humans, rats, and mice. Trans-acting factors were identified that either activated or repressed *Bril*, and evidence indicates that CpG methylation is an epigenetic mode of regulation for *Bril*.

[2] P. Moffatt, unpublished data.

[3] The abbreviations used are: OI, osteogenesis imperfecta; rIHH, recombinant Indian hedgehog; E*n*, embryonic day *n*; Luc, luciferase; PMP, purmorphamine; qPCR, quantitative real-time PCR.

EXPERIMENTAL PROCEDURES

Cell Cultures and Treatment—The HEK293, UMR106, and MC3T3-E1 (subclone 4, hereafter designated MC3T3) cells were obtained from ATCC and used up to passage 16. HEK293 and UMR106 cells were grown in DMEM, and MC3T3 cells were grown in α-minimum essential medium, all supplemented with 10% fetal bovine serum (FBS) (Invitrogen). For transient transfection experiments, cells were seeded at 100,000 cells/well in 12-well plates (Corning). For differentiation of MC3T3, cells were seeded at 100,000 cells/well in 6-well plates (Sarstedt) and grown for 72 h, at which point they reached confluence. From this point on, which was considered day 0, cells were fed α-minimum essential medium + 10% FBS supplemented with 50 μg/ml ascorbic acid (Sigma) and 3 mM β-glycerophosphate (Sigma). Medium was changed every 2 or 3 days. A stock solution of purmorphamine (PMP) (Cayman Chemical, Ann Arbor, MI), an agonist of the hedgehog pathway, was prepared in DMSO at a concentration of 10 mg/ml and stored at −20 °C. PMP was diluted in differentiating medium to a final concentration of up to 3 μM. Concentration of DMSO was kept constant at 0.05% (v/v) and was also added to control cells. Treatment with PMP was commenced at day 0 and continued throughout the experiment with freshly added PMP at every medium change. Recombinant Indian hedgehog (rIHH) C28II N terminus (R&D Systems, Minneapolis, MN) was diluted directly into medium at the desired final concentration. Mineralization was monitored by alizarin red staining as described previously (5).

Luciferase (Luc) Reporter Constructs and Expression Plasmids—The oligonucleotides used in this study are listed in supplemental Table 1. The *Bril* gene promoters were amplified by PCR on genomic DNA extracted from mouse MC3T3 cells, rat UMR106 cells, and human HEK293 cells. Amplification was performed on 25 ng of genomic DNA using Phusion DNA polymerase (New England Biolabs) as recommended by the manufacturer. The sizes of the longest genomic fragments were arbitrarily set at −3913, −1327, and −1434 bp for mice, rats, and humans, respectively. The PCR products extended through to the initiator coding ATG of the *Bril* gene and were cloned directionally into the pGL3-basic (Promega) Luc reporter plasmid. The empty pGL3-basic plasmid was used as a negative control. The promoter regions were progressively deleted from their 5′-ends either using unique restriction sites or through PCR-based amplification (see supplemental Table 1). Internal deletions and point mutations were introduced by whole plasmid amplification using Phusion DNA polymerase (New England Biolabs) with phosphorylated primers covering the desired regions, purified on agarose gel, and religated. Plasmids were prepared using the Midiprep Qiafilter kit (Qiagen). The identity of all constructs was confirmed by Sanger sequencing on an Applied Biosystems 3730xl DNA Analyzer through the McGill University and Genome Quebec Innovation Centre. For co-transfection studies, all effector transcription factors were overexpressed from plasmids under the regulation of the human CMV promoter, except for AP2α, which was an Rous sarcoma virus-driven promoter. The following plasmids were purchased from Origene: human Sp3 variant 1 (Sp3-L1)

(rc222027), human Sp3 variant 2 (Sp3-L2) (rc220658), human LEF1 (rc208663), human DLX5 (sc320170), human OSX (osterix) (sc306509), human HIFα (sc119189), human MSX2 (sc118633), human SOX9 (rc208944), mouse Nfi-X (mc200098), mouse Elk1 (mc201893), mouse Zfp354c (mc203431), mouse Zfp521 (mc204047), mouse Hoxa10 (mc206653). The plasmid encoding the short Sp3 isoform (Sp3-S) was generated by digestion of the Sp3-L1 plasmid with BamHI and MfeI, and ends were blunted with T4 DNA polymerase and religated. Other plasmids were obtained from Addgene (Cambridge, MA): human GLI1 (16419), human GLI2 (17648), human GLI3 (16420), human AP2α (12100), and human cMYC (16011). The cDNAs for GLI1 and GLI3 were excised from their original pBluescript plasmids and subcloned into pCMV6-Neo (Invitrogen). The cDNAs for mouse β-catenin (*βCat*), mouse *Sp1*, and mouse *Tcf7* (encoding the TCF1 protein in mice) were obtained by RT-PCR on RNA from MC3T3 with gene-specific primers (supplemental Table 1). Constitutively active βCat was created by consecutively introducing point mutations in codons for serine 33, serine 37, and threonine 41, which were all converted to alanine residues. Expression plasmids for mouse RUNX2 and ATF4 were obtained from Dr. Gerard Karsenty (Columbia University), and expression plasmids for human MEF2C and MEF2D from Dr. Xiang-Jiao Yang (McGill University). The GFP-expressing plasmid pQBIfc3 (Qbiogene) was used as a negative control.

Transient Transfection and Luc Assays—24 h after seeding, medium was changed, and cells were transfected with Fugene 6 or X-tremeGENE 9 (Roche Applied Science) according to the manufacturer's instructions. The plasmid DNA/transfection agent ratios were 3:1 for HEK293 and UMR106 and 6:1 for MC3T3. For single transfections in UMR106 cells, 400 ng of Luc reporter plasmid was transfected. For co-transfection studies, a plasmid mix containing 100 ng of reporter and 300 ng of effector were used. For triple co-transfections, the reporter plasmid (100 ng) was mixed with effector plasmids to a total of 300 ng, and when necessary, the effector mix was completed with plasmid encoding GFP. 42 h after transfection, 250 μl of passive cell lysis buffer (Promega) was added per well, and Luc activity was measured using 5 μl of cell extract with 100 μl of the luciferase assay system (Promega) on a Sirius luminometer (Berthold, Oak Ridge, TN). Each transfection was done on duplicate wells and repeated at least three times. As negative controls, the empty pGL3-basic or the GFP-expressing plasmids were used to calculate the -fold induction. Mean values with S.E. are either reported as raw relative luciferase units measured or by -fold induction relative to controls.

RNA Extraction, Reverse Transcription, and Real-time qPCR—Cells were washed twice with PBS, and total cellular RNA was extracted with TRIzol (Invitrogen). Purified RNA was quantified on a NanoDrop spectrophotometer (Thermo Scientific), and 2 μg was reverse transcribed in 20 μl with the High Capacity cDNA synthesis kit (Applied Biosystems). Real-time qPCR was performed on an Applied Biosystems 7500 PCR machine with 0.5–1 μl of cDNA in a 25-μl reaction volume with the 2× Universal PCR Master Mix and the following Taqman probes (Applied Biosystems): *Alp* Mm00475834_m1, *Bglp1* (osteocalcin) Mm03413826_mH, *Gli1* Mm00494654_m1, *Gli2* Mm01293116_m1, *Gli3* Mm00492345_m1, *Bril* Mm00804741_g1, *Mef2c* Mm01340842_m1, *Runx2* (Runt-related transcription factor 2) Mm00501584_m1, *Sp1* Mm00489039_m1, *Sp3* Mm00803425_m1, *Osx* Mm00504574_m1, *Tcf7* Mm00493445_m1, *Zfp354c* Mm00457419_m1. All data are normalized to *β-actin* (4352933) or ribosomal *18S* (Mm03928990_g1), and values were expressed as $2^{-\Delta}C_t$ (28).

Alkaline Phosphatase Activity and Western Blotting—Alkaline phosphatase (ALP) activity was measured on cell extracts prepared with 100 mM Tris-HCl (pH 9.0) containing 0.1% Triton X-100. Extracts were mixed with *p*-nitrophenyl phosphate (Sigma), and the activity was recorded on an ELx808 96-well microplate reader (BioTek) at 450 nm over 60 min at 37 °C with readings every 5 min. Protein concentrations were measured using the Bradford reagent (Bio-Rad), and specific activity (*p*-nitrophenol phosphate produced/min/mg of protein) was calculated using a standard curve of *p*-nitrophenol (Sigma). For Western blotting, total cell extracts were prepared with 50 mM Tris-HCl (pH 7.4), 150 mM NaCl, 1 mM EDTA, 1% (v/v) Nonidet P-40. Insoluble material was pelleted at 13,000 rpm for 10 min at 4 °C, and the supernatant was mixed with 4× Laemmli buffer and boiled. SDS-PAGE and Western blotting were performed as described previously (5). Equal amounts of protein loaded across lanes were verified by immunoblotting with an anti-ACTIN antibody (clone MA1-744) from Affinity BioReagents (Golden, CO). The anti-BRIL antibody was as described previously (5).

Mapping of Transcriptional Start Sites—The transcription start sites of the mouse and rat *Bril* gene were mapped using the oligonucleotide-capping 5′-rapid amplification of cDNA ends strategy as described previously (1, 29). Briefly, total RNA was extracted from differentiating mouse MC3T3 cells at day 15 and confluent rat UMR106 cells. Poly(A) RNA was purified using the OligoTex kit (Qiagen) and processed as follows. mRNAs were dephosphorylated with bacterial alkaline phosphatase (Takara) and then treated with tobacco acid pyrophosphatase (Epicenter Biotechnologies) to remove the cap structure. An RNA linker was ligated with T4 RNA ligase 1 (New England Biolabs) at the 5′-end of mRNA. The purified RNA was reverse transcribed with SuperscriptIII (Invitrogen) and the Bril-specific reverse primer. The cDNA was then amplified by PCR using a forward primer complementary to the RNA linker and a nested reverse primer specific for *Bril*. The PCR products were separated on a 1.5% agarose gel, purified from gel on Minelute columns (Qiagen), and cloned into pBluescript plasmid. Plasmids were purified from cultures of bacterial transformants, and DNA was sequenced with T7 primer.

DNase I Footprinting and Electromobility Shift Assay (EMSA)—Nuclear extracts used for both DNase I footprinting and EMSA were prepared from HEK293 cells based on a previously published technique (30). Extracts were obtained 48 h after transient transfection or not with plasmid expressing Sp1 in HEK293. The procedure for the DNase I footprinting assay was essentially as described (31, 32). To generate a rat *Bril* promoter DNA probe, an oligonucleotide covering positions −265 to −247 relative to the ATG was end-labeled with T4 polynucleotide kinase (New England Biolabs) and 50 μCi of [γ-^{32}P]ATP (3000 Ci/mmol) (PerkinElmer Life Sciences) at

37 °C for 1 h. Using the rat *Bril* promoter Luc construct as template, a PCR fragment was amplified with the labeled primer and a reverse primer located at 66 bp within the coding region of Luc. The resulting 331-bp fragment was purified on a 5% acrylamide-TBE gel, and 25,000 cpm was used for binding with nuclear extracts at 25 °C for 10 min. Increasing concentrations of HPLC-pure DNase I (Amersham Biosciences) were added and digested for exactly 2 min at 25 °C. The reaction was stopped and treated with proteinase K for 30 min at 55 °C. After precipitation, the digested probe was separated on a 5% acrylamide-urea-TBE sequencing gel. Gel was dried and exposed to radiography film for 18 h at −80 °C. The naked probed without nuclear extracts was digested in parallel and ran side-by-side on the gel. A Maxam-Gilbert G + A chemical sequencing reaction on the labeled probe was performed to obtain a proper ladder. For EMSA, oligonucleotide pairs were end-labeled as above with [γ-^{32}P]ATP, annealed, and purified on Illustra ProQuant G50 microcolumns (GE Healthcare). Labeled double-stranded oligonucleotides (50,000 cpm; 13 fmol) were incubated with nuclear extracts for 10 min at 25 °C and separated on 4% acrylamide-TBE (0.5×) gels. Gels were dried, and autoradiography was performed for 3–15 h.

Gli2 Knock-out Mice and Tissue Processing—All animal experimentation was reviewed and approved by the Shriners Hospital for Children animal care committee and McGill University. The *Gli2* heterozygote mice were kindly provided by Dr. Janet Henderson (McGill University) and maintained in the C3H background. The *Gli2*$^{-/-}$ mice were described previously to be perinatally lethal and shown to have impaired bone development (33, 34). In order to generate the *Gli2*$^{-/-}$ embryos at defined stages, heterozygote mice were intermated, and detection of vaginal plugs was determined as being E0.5. At embryonic stages E15.5 and E17.5, pregnant females were euthanized by CO_2 asphyxia followed by cervical dislocation. Embryos were dissected, and genomic DNA was extracted from tails for PCR genotyping exactly as described previously (33, 34). Hind limbs and heads were dissected and processed for RNA extraction and immunohistochemistry. The hind limbs were skinned and homogenized with a Polytron homogenizer into 1 ml of TRIzol, and total RNA was extracted and processed for RT-qPCR as described above. For immunolocalization of BRIL, hind limbs were fixed with 4% paraformaldehyde in phosphate buffer (0.1 M, pH 7.0) at 4 °C for 24 h, washed with PBS, and decalcified (only for E17.5 tissues) at 4 °C for 48 h with a 15% EDTA solution (pH 7.0). After dehydration, tissues were embedded into paraffin, and 5-μm sections were cut. All subsequent steps were performed at room temperature. Sections were deparaffinized with xylenes and rehydrated. Sections were sequentially incubated with dual endogenous enzyme block (Dako) for 10 min, 5% skim milk in PBS for 1 h, and anti-Bril affinity-purified antibody (0.02 μg/ml) in PBS with 0.5% skim milk for 1 h. Sections were washed five times with PBS, incubated with Envision+ anti-rabbit HRP polymer (Dako) for 30 min, and washed five times with PBS. Visualization was achieved by incubation with the Liquid DAB+ Substrate Chromogen system (Dako) for 10 min and then rinsing thoroughly with tap water. Sections were briefly counterstained with hematoxylin QS (Vector) and mounted with Microkitt (Macalab). Photographs were taken on a Laica microscope equipped with an Olympus DP70 digital camera.

Bisulfite Sequencing and in Vitro Methylation of Plasmids—MC3T3 cells were grown to confluence and differentiated for 3 days in the absence or presence of 1 μM PMP. Total genomic DNA was isolated and purified. 2 μg of genomic DNA from control and PMP-treated cells were treated using the MethylCode Bisulfite Conversion Kit (Invitrogen) and subsequently purified as recommended by the manufacturer. Converted genomic DNA was then amplified by PCR using two different primer pairs designed with the MethPrimer software (35). The primer sequences are matching fully converted DNA, where all Cs have been converted to Ts, and do not cover any CpG dinucleotides. They amplify two overlapping fragments of the mouse *Bril* gene of 172 and 250 bp. In total, the analysis looked at 12 CpG sites located on a 408-bp segment starting from −242 to +166 in relation to the ATG (position set as +1). Each PCR contained 600 ng of converted genomic DNA, a 0.5 μM concentration of each primer, 0.2 mM dNTP, 3 units of recombinant TaqDNA polymerase (New England Biolabs) in a final reaction volume of 25 μl. The PCR program was as follows: 95 °C for 2 min (one cycle); 94 °C for 30 s, 56 °C for 25 s, 72 °C for 25 s for 35 cycles. The PCRs were loaded on a 2% agarose gel, stained with ethidium bromide, and the products were excised from the gel and purified on Minelute columns (Qiagen). The purified products were then ligated into pBluescriptKS having T/A overhangs. After transformation into DH10B bacteria, randomly selected colonies were picked for plasmid preparation. Sequencing was done with the T7 primer on a total of 72 independent clones (18 each for the control and PMP-treated cells, for both primer pairs). The human −1434 bp promoter Luc reporter plasmid was methylated *in vitro* using the M.SssI CpG methyltransferase (New England Biolabs). Briefly, 6 μg of plasmid was incubated for 4 h at 37 °C in a final volume of 120 μl with 40 units of M.SssI in the presence of 160 μM *S*-adenosylmethionine. As control, the plasmids were processed under identical conditions but without enzymatic treatment. The treated and non-treated plasmids were purified on Minelute columns (Qiagen) and digested with HpaII (cleavage inhibited by methylation) or MspI (cleavage insensitive to methylation) to confirm the methylation efficiency. Plasmids (100 ng) were then co-transfected into HEK293 cells together with 300 ng of either GFP or Sp1. Luc activity was assayed 42 h later.

RESULTS

Characteristics of the Bril Gene and Promoter Region—In order to search for potential regulatory regions present in the vicinity of the *BRIL* gene and common between humans (Fig. 1*A*), rats, and mice, the genomic sequences were analyzed *in silico* using the ECR Browser (available on the World Wide Web). The highest regions of similarity found were those covering the exons and intron (Fig. 1*B*). A very high region of identity (*red area*, up to 75%) was also observed on a short stretch upstream of exon 1 covering about 400 bp, which probably corresponds to the proximal promoter (Fig. 1*C*). Further upstream, the sequence homology abruptly became very divergent and less likely to contain conserved regulatory elements. Another highly conserved region covering about 70 bp was also identi-

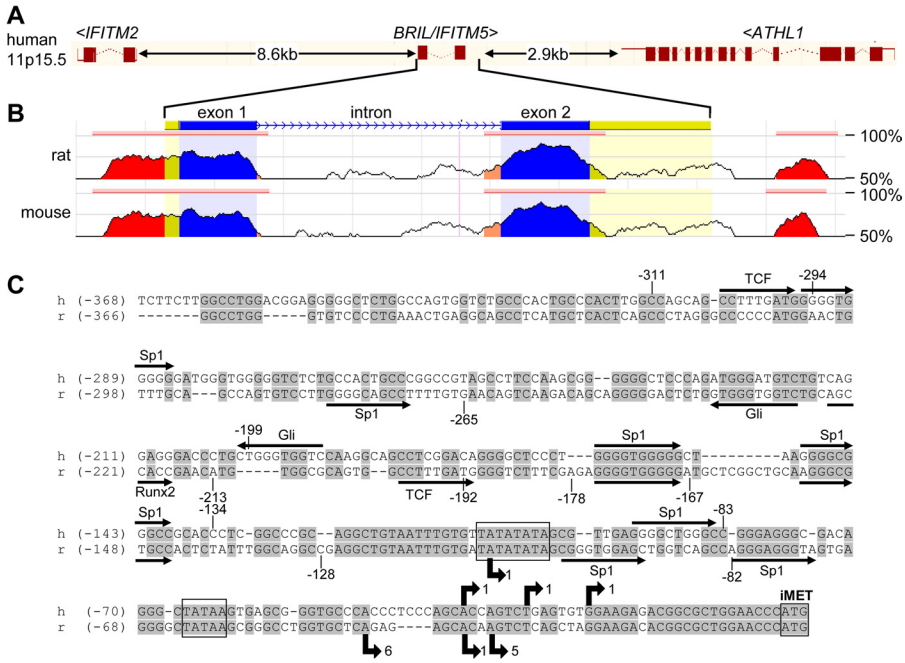

FIGURE 1. **Structure, conservation, and promoter region annotation of the human and rat *Bril* genes.** *A*, schematic representation of the human *BRIL* gene locus, flanked with the *IFITM2* and *ATHL1* genes. *B*, evolutionarily conserved regions between the human and the rat and mouse genes are graphically represented. Plots illustrate regions with the highest degree of similarity (percentage indicated at the *right*) for the genomic sequence of rats and mice as compared with humans (*top*). The regions indicated in *red* cover the putative promoter (*left*) and the 3′-intergenic region (*right*). *C*, sequence alignment of the human (*h*) and rat (*r*) genomic sequences extending about 360 bp upstream of the coding ATG in exon 1. Transcriptional start sites are indicated by *bent arrows below* and *above* the sequences for rats and humans, with *numbers* indicative of transcripts sequenced. Identical bases are *shaded gray*, and putative TATA elements are *boxed*. Conserved putative binding sites for transcription factors are represented by *arrows*.

fied in the 3′-intergenic region (*red area*). The transcriptional start site for rats was experimentally mapped using oligonucleotide-capping methodology in UMR106 cells. The results indicated that transcription initiates at different sites, with a variable 5′-untranslated region of about 70–100 bp (Fig. 1*C*, *bent downward arrows*). Very similar results were observed in mice, where transcription start sites in MC3T3 cells are within 70 bp upstream of the coding ATG (data not shown). For human *BRIL*, inspection of expressed sequence tags found at UniGene (available on the NCBI, National Institutes of Health Web site) revealed the transcription start sites clustered at around −30 bp relative to the ATG (Fig. 1*C*, *bent upward arrows*). Among the putative DNA regulatory element transcription factor binding sites found most frequently, irrespective of species, were Sp1-like, GC-rich binding sites (Fig. 1*C*). At least four such GC-rich sequences are present within the proximal promoters of rats, humans, and mice. This is perhaps not inconsistent with the high GC content (70%) feature of this region being annotated as a CpG island in the human *BRIL* gene. Of special interest was also the presence of elements matching the binding site for GLI, TCF/LEF, and two putative TATA boxes (Fig. 1*C*, *boxed*). Other putative elements for ZFP354c, AP2α, and RUNX2 were also variably found interspersed in rats, humans, and mice.

Mapping of Rat and Human Bril Promoter Regulatory Elements in UMR106 Cells—In order to map the regulatory regions important to drive expression of *Bril* gene transcription, genomic fragments for mice (−3913), rats (−1327), and humans (−1434) were cloned in the pGL3-basic Luc reporter plasmid. Transient transfection experiments were first conducted in osteosarcoma UMR106 cells (Fig. 2) that were found to express *Bril* constitutively (5). The activities of all full-length promoter constructs tested were highly active in UMR106 cells (~300,000 relative light units) as compared with the empty pGL3-basic plasmid (~20,000 relative light units). Progressive deletions from the 5′-end of the promoter fragments indicated a significant loss of activity at −213 for rats (Fig. 2*A*, *gray bars*) and at −134 for humans (Fig. 2*B*, *gray bars*). The activity further declined to background levels for the −82 and −53 fragments (Fig. 2, *A* and *B*). Internal deletions covering the same regions displayed a similar loss in activity (Fig. 2, *A* and *B*, *black bars*). These data suggested that crucial regulatory elements are located within ~250 bp upstream of the ATG. Very similar results were obtained with the mouse *Bril* promoter region, and longer upstream sequences up to 3.9 kb did not afford more activity to the promoter (supplemental Fig. 1).

Sp1 Binds Several Rat Promoter GC-rich Elements in Vitro—Because of the high GC-rich content of the promoter region, we further investigated whether the Sp1 transcription factor could physically interact with the rat proximal fragment *in vitro* using DNase I footprinting and EMSAs (Fig. 3). A rat −283 bp end-labeled fragment was incubated or not (nude probe) with nuclear extracts prepared from wild type or HEK293 cells transiently transfected with an Sp1 expression plasmid. Upon incubation with Sp1-containing nuclear extracts, the rat promoter clearly showed three protected regions (Fig. 3*A*; *labeled FP1*, *FP2*, and *FP3*), which mapped to three GC-rich sequences as determined by Maxam-Gilbert sequencing (indicated at the *left* in Fig. 3*A*). Partial protection was also noticed on FP1 and FP2 using nuclear extracts from wild type HEK293 cells. To further delineate which rat sequences can interact with Sp1, oligonu-

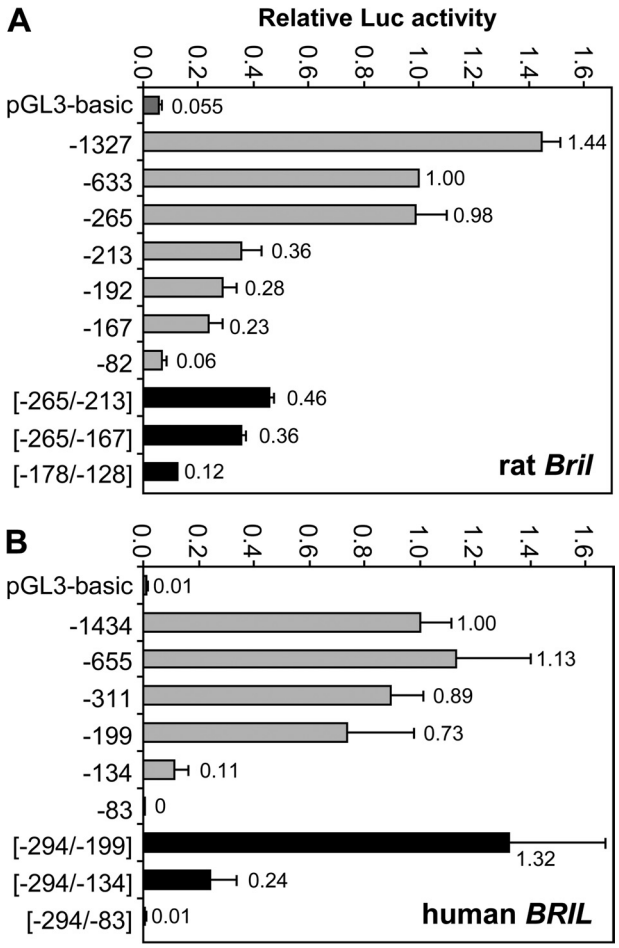

FIGURE 2. **Transcriptional activity of the *Bril* promoter in UMR106 cells.** The rat (*A*) and human (*B*) promoter regions were cloned into the pGL3-basic reporter plasmid, and Luc activity was measured 48 h after transient transfection in UMR106 cells. The longest constructs tested extended 1327 and 1434 bp upstream of the coding ATG for the rat and human, respectively. Progressive truncations from the 5′-end (*gray bars*) and internal deletions (*back bars*) indicated that maximal regulatory activity resides within −265 bp (rat) and −199 bp (human), with complete loss of activity down to −82 bp. Data represent relative Luc activity as compared with the −633 and −1434 bp for the rat and human constructs, respectively. Promoterless pGL3-basic was used as a negative control. Results shown are mean ± S.E. (*error bars*) ($n = 4$).

cleotides containing GC-rich elements (Fig. 3*B*, *top*) were incubated with nuclear extracts from HEK293 cells overexpressing Sp1 and analyzed by EMSA. All oligonucleotides except −117 yielded an Sp1-specific complex (Fig. 3*B*, *bottom*) but with different affinities. Intensity for −160, −142, and −82 was similar to that observed with the oligonucleotide containing the consensus Sp1 binding site (Fig. 3, *Sp1*). The mutant Sp1 oligonucleotide having two mutated bases (Fig. 3, *mSp1*) did not bind Sp1. Interestingly, footprints FP1, FP2, and FP3 observed in Fig. 3*A* matched oligonucleotide sequences −61, −82, −142, and −160, respectively.

Sp Family Members Can Transactivate the Bril Promoters in Vivo—A co-transfection assay was next performed to screen a selected set of transcription factors that could activate the human −1434 bp Luc reporter in HEK293 and MC3T3 cells (supplemental Fig. 2). Among 15 transcription factors tested, Sp1 had some of the strongest transactivating properties. To further determine whether other Sp family members could activate the *Bril* promoters for rats (−1327), mice (−1630), and humans (−1323), they were co-transfected with Sp1, Sp3, or OSX in MC3T3 (Fig. 4*A*) and HEK293 (Fig. 4, *B* and *C*). Three different isoforms of Sp3 (Sp3-L1 (residues 1–781), Sp3-L2 (residues 69–781), and Sp3-S (residues 286–781)) were also tested because of the reported stimulatory (Sp3-L1 and Sp3-L2) and inhibitory effects (Sp3-S). In both cell types, the *Bril* promoter activity was most dramatically induced by Sp3-L1 > Sp1 > Sp3-L2, to more than 60- and 700-fold relative to the negative GFP control, in MC3T3 (Fig. 4*A*) and HEK293 (Fig. 4*B*), respectively. Sp3-S did not induce a significant increase in activity, whereas OSX only had marginal effects compared with Sp1 and Sp3. OSX was more active in MC3T3 cells, reaching an up to 10-fold increase relative to background for the human promoter (Fig. 4*A*). Of note is the extremely high -fold increase attained in HEK293 cells compared with MC3T3, probably reflecting much better transfection efficiencies in HEK293 (>50%), in contrast to MC3T3 (<5%). The effects of combinations of Sp1 with other Sp members on the activity of the human *BRIL* promoter were also tested in HEK293 (Fig. 4*C*). Two important findings were observed. First, doubling the amount of transfected Sp1 (from 150 to 300 ng) resulted in the promoter being 3.7-fold more active, suggesting a synergistic mode of activation. Second, co-transfection of Sp1 with Sp3-L1, Sp3-L2, and surprisingly Sp3-S or OSX also resulted in -fold inductions greater than simple additive effects. These data suggest that Sp members are potent transactivators of *Bril* and that they potentially interact together and with OSX to give synergistic effects.

Contribution of TATA Boxes and Individual Sp1 Elements to Bril Promoter Activity—The human *BRIL* promoter was selected for subsequent studies because of its higher responsiveness to transcriptional regulators, at least of the Sp family. We next analyzed the contribution of the two TATA-like boxes and of the four Sp1-like sites. To abolish activity of the respective elements, as depicted in Fig. 5*A*, we introduced either internal deletions in the putative TATA boxes or two point mutations in the Sp1 elements that abolished binding activity (see Fig. 3*B*). Co-transfection experiments were performed in HEK293 cells to assess the base-line (with GFP) and stimulated (with Sp1) activity of the human −452 promoter, which retains full activity compared with the −1434 bp promoter (see Fig. 1*B*). Deletion of the proximal TATA (Δ-pTATA) caused a 67% decrease in base-line activity (Fig. 5*B*, *left*). Induction by Sp1 was also dramatically reduced in the construct lacking the proximal TATA box (Fig. 5*B*, *right*). Deletion of the distal TATA box (Δ-dTATA) did not impact the base-line and Sp1-induced activity of the reporter (Fig. 5*B*). The constructs carrying single, double, triple, or quadruple mutations in the four Sp1 elements were tested for activation by Sp1 in HEK293 cells (Fig. 5*C*). Each of the four sites contributed to a different extent to Sp1 responsiveness, with site 1 (at −83) and sites 2, 3, and 4 contributing to about 60 and 25% of the reporter activity, respectively. The double and triple site mutants had activities ranging from 50% to more than 80% reduction in activity, whereas the quadruple mutant had less than 10% of residual activity (Fig. 5*C*). These data suggest that induction by Sp family members is dependent on the presence of multiple binding sites in conjunction with the proximal TATA box.

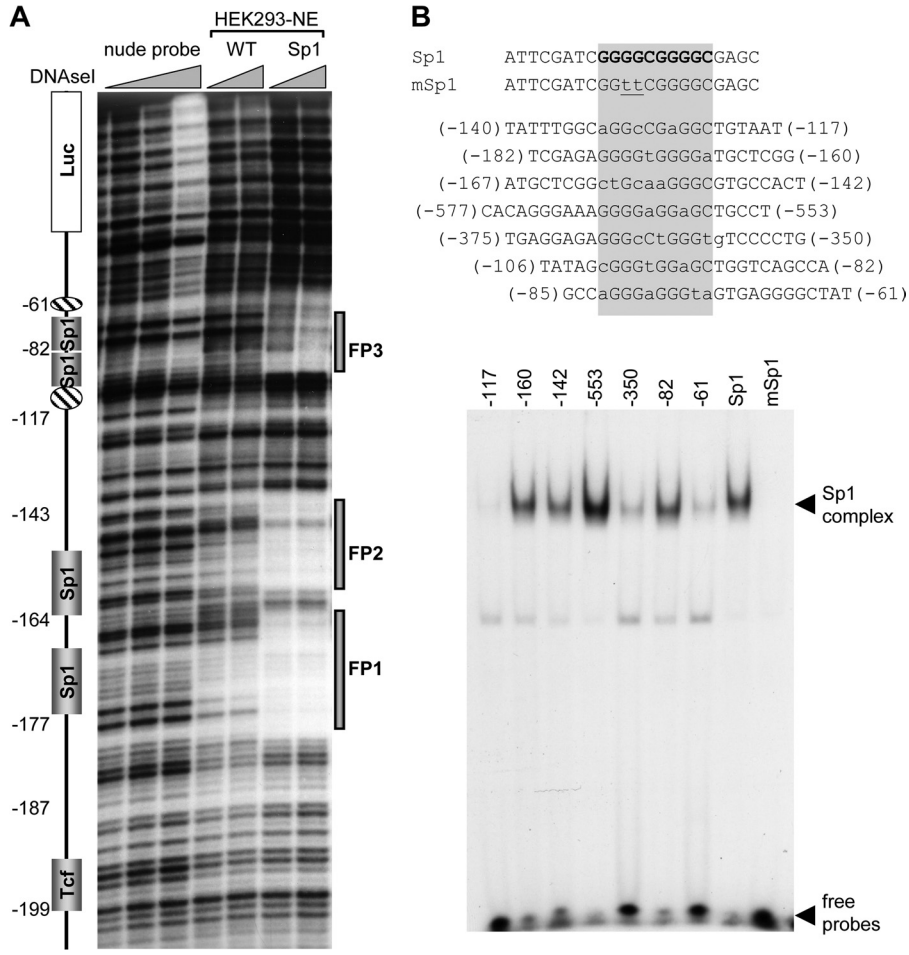

FIGURE 3. **Sp1 binds to multiple elements in the rat *Bril* promoter.** *A*, DNase I footprinting analysis was performed on the rat −265 bp probe end-labeled with ^{32}P and incubated in the absence (nude probe) or presence of nuclear extracts (*NE*) from WT HEK293 cells or HEK293 cells overexpressing Sp1. The DNA-protein complex was then digested with increasing amounts of DNase I. Samples were loaded on sequencing gels and autoradiographed. The DNA ladder indicated at the *left* was prepared by chemical G + A Maxam-Gilbert sequencing (not shown). The three regions protected by Sp1 (*FP1*, *FP2*, and *FP3*) correspond to the GC-rich elements identified and annotated at the *left* (see also Fig. 1*C*). *B*, EMSA was performed with different ^{32}P-labeled double-stranded oligonucleotides (*top*) covering different regions of the rat *Bril* promoter. The central core (*boxed*) *highlights* the putative Sp1 binding sites, with mismatches to the consensus Sp1 sequence indicated in *lowercase letters*. A mutant Sp1 probe (*mSp1*) having 2 nucleotide mismatches served as a negative control. Probes were incubated with nuclear extracts from HEK293 cells overexpressing Sp1, separated on PAGE, and visualized by autoradiography.

Zfp354C Can Repress Base-line and Sp1-mediated Activation—The *in silico* search for potential binding sites of the *Bril* promoter revealed the presence of several consensus binding sites (CCAC) for ZFP354C. For instance, in the proximal promoter segments shown in Fig. 1*B*, there are 10 and 8 potential CCAC elements, respectively, for humans and rats. This is of particular interest because ZFP354C (also called KID3A and AJ18) is a C2H2 zinc finger transcription factor of the KRAB (Kruppel-associated box) family, known for its general repressive functions on transcription, particularly on RUNX2-mediated regulation of the osteocalcin promoter in osteoblasts. When tested on the rat, mouse, and human promoter segments, Zfp354C systematically repressed the base-line activity in HEK293 cells down to as much as 76% (Fig. 6*A*). In a co-transfection experiment in HEK293 cells, ZFP354C was also found to be a potent inhibitor of Sp1-mediated transactivation of the human −1434 bp promoter (Fig. 6*B*). A plasmid ratio of ZFP354C/Sp1 as low as 1:6 (25 ng/150 ng) significantly reduced the induction by 25% (Fig. 6*B*). More robust inhibitory effects were observed with progressively increasing ZFP354C/Sp1 ratios, up to 99% repression at equal quantities (Fig. 6*B*). Expression of *Zfp354C* measured by RT-qPCR was 60-fold greater in cells not expressing endogenous *Bril* (HEK293 and NIH3T3) relative to those expressing (UMR106) or committed to express it (MC3T3) (data not shown).

The Conserved 3′-Intergenic Region of BRIL Is Not a Direct Target of Runx2—Consistent with the absence of the canonical RUNX2 binding site (ACCACA) within the promoter region of *Bril*, the human −1434 bp promoter was not inducible by RUNX2 (supplemental Fig. 2). However, a highly conserved segment of genomic DNA located in the 3′-intergenic region (Fig. 1*B*) was found to contain two perfect RUNX2 binding elements located 172 and 246 bp downstream of the 3′-UTR region (supplemental Fig. 3*A*). To test the possibility that these sites might be functionally operative, the synthetic SV40 polyadenylation cassette of the human −1434 bp Luc reporter construct was replaced with the entire 3′-UTR region, including 289 bp of the intergenic region of the human *BRIL* gene (supplemental Fig. 3*B*). The activity of this "natural" *BRIL* 3′-UTR and downstream elements remained at base-line levels after

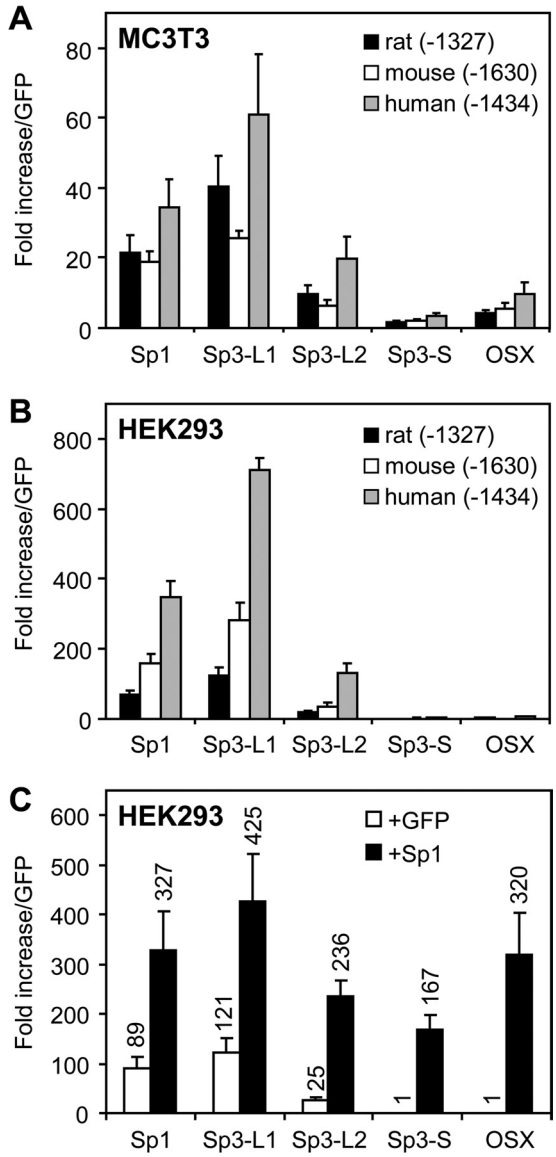

FIGURE 4. **Transcriptional activation of the rat, mouse, and human *Bril* promoter by Sp family members.** The promoter Luc constructs (100 ng) were co-transfected with 300 ng of each expression plasmids encoding Sp1, Sp3-L1 (long form 1), Sp3-L2 (long form 2), Sp3-S (short form), and OSX. Luc activity was measured 48 h after transient transfection into MC3T3 osteoblasts (*A*) or HEK293 (*B* and *C*). *C*, the human −1434 bp promoter Luc construct (100 ng) was co-transfected with 150 ng of each plasmid encoding either GFP or Sp1, in combination with the other Sp members. The *first two bars* represent transfection of Sp1 (150 ng) with GFP (150 ng) or with itself (300 ng). Results are presented as -fold increase relative to the negative control plasmid encoding GFP. Results shown are mean ± S.E. (*error bars*) (n = 3–5).

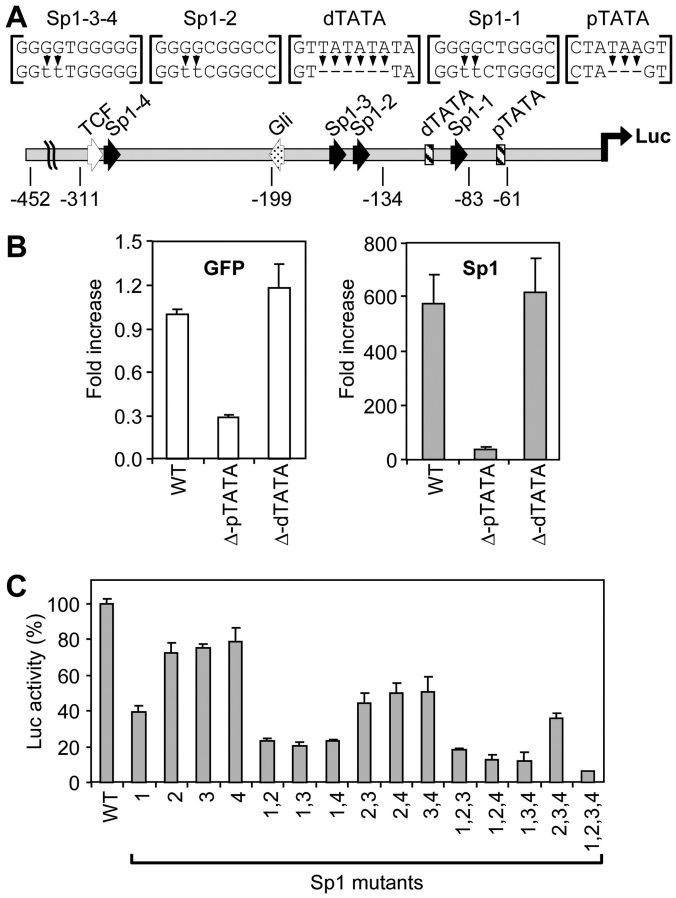

FIGURE 5. **Contribution of the putative TATA boxes and Sp1-like elements to the activity of the human *BRIL* promoter.** *A*, schematic diagram depicting the −452 human *BRIL* promoter with some elements highlighted. Deletions and point mutations were introduced in each of the two putative TATA boxes (proximal and distal, *hatched boxes*) and the four Sp1-like elements (*black arrows*, *labeled Sp1-1* to *Sp1-4*), as illustrated at the *top*. WT and mutant human *BRIL* Luc constructs (100 ng) were co-transfected with either GFP or Sp1 expression plasmids (300 ng) in HEK293 cells. Luc activity was assayed 48 h later and plotted relative to the activity of the WT promoter. *B*, deletion of the proximal TATA box significantly attenuates both basal (*left*) and Sp1-induced (*right*) *BRIL* promoter activity. *C*, the effect of mutation of the four Sp1 sites (*1–4*) were tested individually and in different combinations (double, triple, quadruple), in co-transfection with Sp1. The activities of the various Sp1 mutants are expressed as a percentage of maximal activity of the WT. Results shown are mean ± S.E. (*error bars*) (n = 3).

co-transfection with a RUNX2 expression plasmid, suggesting that this region was not functional at least in this plasmid configuration (supplemental Fig. 3). The *BRIL* 3′-UTR plasmid was still fully responsive to Sp1 (supplemental Fig. 3).

GLI2 Regulates Bril in Conjunction with Sp Members in MC3T3—Another putative element identified in the *Bril* promoter is a canonical binding site for the GLI transcription factors, located in the reverse orientation at −191 and −228 in humans and rats, respectively (Fig. 1*B*). The consensus binding site for GLI has a core of 10 nucleotides (GACCACCCAC-NNNG) (Fig. 7*A*, *top*), which becomes a high affinity site when a G is present at +4 relative to the core (36, 37). The human site is an almost perfect match to the high affinity consensus except for a single base change at the last position of the core, which is known to be divergent at that position (GACCACCCAGcagG). The rat GLI site also is a perfect match except at the +4 G (GACCACCCACcagA). The functionality of the GLI site to the activity of the human promoter was tested by co-transfection experiments in MC3T3 (Fig. 7*A*). The wild type human −1434 bp promoter was responsive to all three human Gli family members but with the following magnitude of potency: GLI2 ≫ GLI3 > GLI1 (Fig. 7*A*). The −1434 bp promoter having two point mutations introduced within the GLI binding element (Fig. 7*A*, *top*), became unresponsive to GLI1 and GLI3 but was still slightly activated (~3-fold) by GLI2. Another putative GLI site located further upstream at position −763 (GACCACtCACcacA), could have contributed to this residual activity, but this was not investigated.

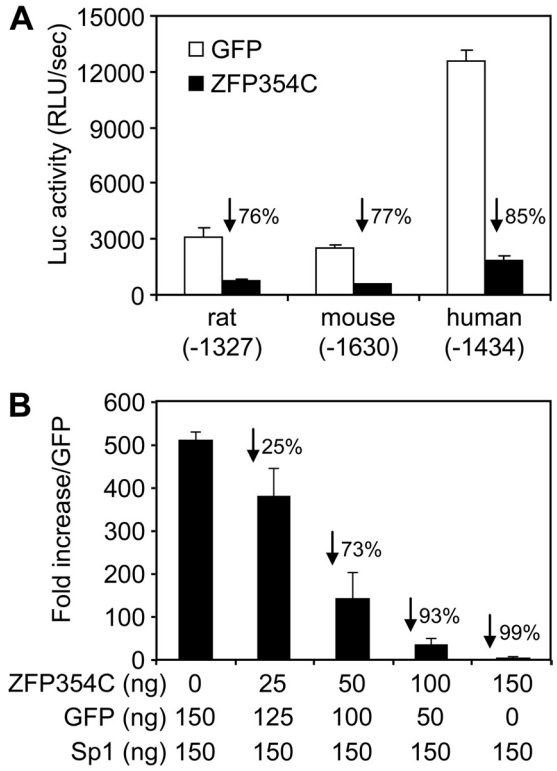

FIGURE 6. **ZFP354C represses basal and Sp1-induced transcriptional activity of the *Bril* promoters.** *A*, the rat, mouse, and human promoter Luc constructs (100 ng) were co-transfected in HEK293 cells with GFP or ZFP354C expression plasmids (300 ng). Luc activity was assayed 48 h later, and the raw values are presented. ZFP354C repressed the base-line Luc activity for the three species from 76 to 85%. *B*, the human −1434 bp promoter construct (100 ng) was co-transfected with a fixed amount of Sp1 (150 ng) and with increasing quantities (0, 25, 50, 100, and 150 ng) of ZFP354C. The amount of co-transfected plasmid was kept constant at 300 ng with GFP. The values represent the -fold increase relative to co-transfection with GFP alone (300 ng). Results shown are mean ± S.E. (*error bars*) ($n = 3$).

To further delineate the responsiveness of the human *BRIL* promoter to GLI2, a kinetic and dose-response experiment was performed in MC3T3 (Fig. 7*B*). Activity of the human −1434 bp promoter to GLI2 was significantly different in both the kinetics and magnitude of induction as compared with Sp1 (Fig. 7*B*), peaking at 15 h post-transfection with an increase up to 80-fold. The potency of GLI2 was greater than Sp1, with significant induction being detected with only 50 ng of plasmid transfected, above those recorded at 15 and 25 h for Sp1 used at 300 ng (Fig. 7*B*, *filled symbols*). Co-transfection of GLI2 with either OSX or Sp1 also resulted in activities that were significantly higher than the sum of individual responses (Fig. 7*C*), suggesting again a synergistic control of *BRIL* activation. This was not a generalized response because TCF1, when used in combination with GLI2, did not significantly affect its transcriptional readout. Last, endogenous *Bril* expression in MC3T3 transfected with GLI2 was significantly increased by 2.7-fold at 25 h (Fig. 7*D*), suggesting that GLI2 can directly modulate *Bril*.

Hedgehog Signaling in MC3T3 Stimulates Bril Expression, Differentiation, and Mineralization—We next confirmed whether activation of the hedgehog signaling pathway, which leads to GLI2 activation, could regulate endogenous *Bril* expression in osteoblasts. MC3T3 cells were grown to confluence (day 0) and incubated in differentiating media in the absence or presence of PMP. PMP is a direct agonist of Smoothened (SMO), the transmembrane receptor that ultimately transmits intracellular signals to modulate gene expression through GLI transcription factors. SMO is normally kept in check by the repressive action of another transmembrane protein called Patched (PTCH), the receptor of hedgehog proteins. Hedgehog binding to PTCH relieves the inhibition of SMO, the signaling effector of the cascade. MC3T3 continuously treated with 1 μM PMP had an accelerated mineralization, as determined by alizarin red staining (Fig. 8*A*). Compared with control cells receiving DMSO only, which started mineralizing at around day 10, PMP-treated cells displayed almost maximal alizarin red staining at day 7 and continued to increase at day 10. ALP activity was also induced 2–9-fold starting on day 2 after treatment (Fig. 8*B*). Western blotting also revealed markedly increased levels of BRIL from day 2 onward (Fig. 8*C*), when levels of BRIL in control cells are still undetectable. Maximal expression of BRIL peaked at day 4, as compared with days 7 and 10 for the untreated cells. The effect of PMP on BRIL at day 4 was also concentration-dependent, being effective as low as 0.3 μM and maximal at 3 μM (Fig. 8*D*, *left*). Treatment of MC3T3 for 4 days with rIHH also induced strong expression of BRIL at both concentrations tested (Fig. 8*D*, *right*), suggesting that the entire PTCH-SMO axis was operative.

Gene Expression Pattern in MC3T3 Treated with PMP—The gene expression signature of control and PMP-treated MC3T3 was investigated in more detail by qPCR (Fig. 9). In comparison with control cells, the expression of *Bril* was up-regulated 2-, 29-, 33-, and 17-fold at day 1, 2, 3, and 4, respectively. By day 10, *Bril* expression had returned to control levels. The general kinetic pattern of *Bril* transcripts paralleled those observed at the protein level (Fig. 8*D*). This profile of *Bril* expression during MC3T3 differentiation was overall similar to that of markers of differentiation, *Alp* and *Ibsp* (integrin binding sialoprotein) (Fig. 9, *first row*). In contrast, expression of osteopontin (*Ssp1*) and osteocalcin (*Ocn*) were mostly unaffected at the early time points (days 1–4) but increased significantly at days 7 and 10. A subset of transcription factor gene expression was also monitored to see which would correlate with that of *Bril*. Among those tested, *Gli1* was most responsive to PMP and was induced at the earliest time point tested (19-fold at day 1 up to more than 50-fold at days 2, 3, and 4) (Fig. 9, *second row*). *Gli2* also was increased 2-, 13-, and 20-fold by day 1, 2, and 3, respectively. *Gli3* levels remained constant, and more modest increases (2–3-fold) were noted for *Runx2* throughout the experiment. Marginal to no inductions were observed for *Sp1*, *Sp3*, and *Zfp354C*. Interestingly, the *Mef2c* and *Tcf7* transcription factors were also up-regulated by PMP, in the range of 2–10-fold. It should be noted that expression profiles for *Gli2*, *Osx*, *Mef2C*, and *Tcf7* in non-treated cells also increased steadily up to about days 7–10, in a similar fashion to those of *Bril*. These data suggest that PMP promoted gene expression of *Bril* and accelerated differentiation of MC3T3 cells.

Bril Expression Domain Is Reduced in Long Bones of Gli2 Knock-out Mice—In order to verify whether GLI2 is essential for *Bril* expression *in vivo*, we examined the *Gli2* knock-out (KO) mouse model (33, 34), having a deletion in exons encoding for the zinc fingers 3–5. Expression of *Gli2* and *Bril* was

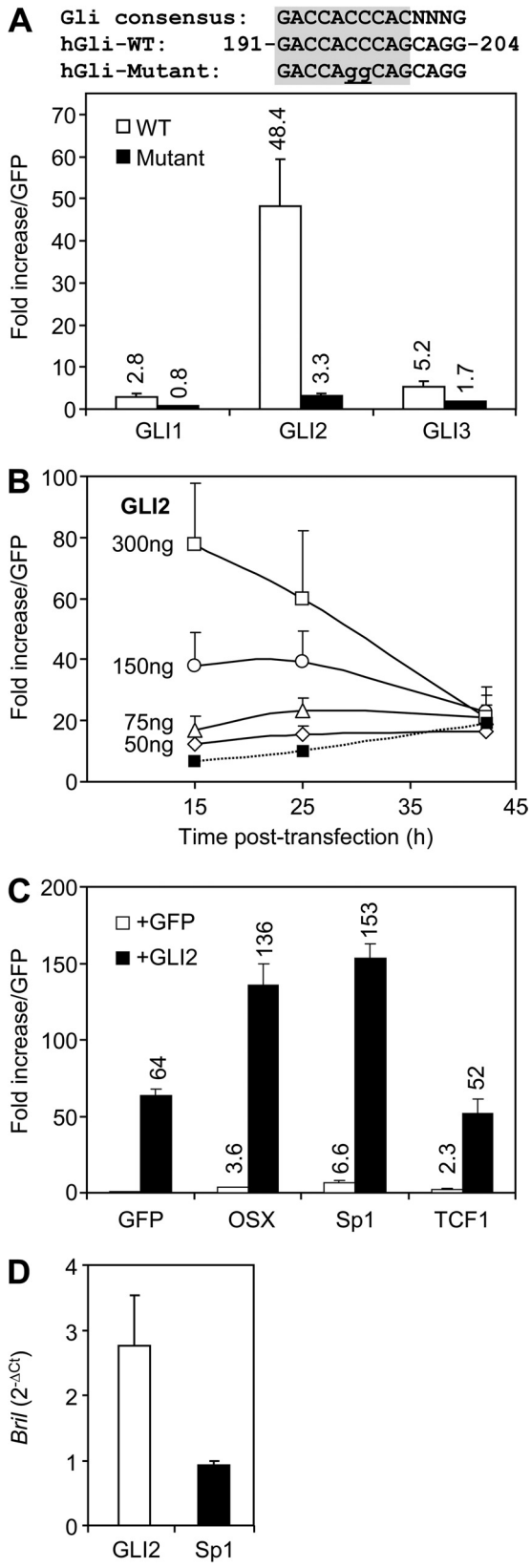

FIGURE 7. **Activation of the human *BRIL* promoter and endogenous mouse *Bril* gene by GLI2 in MC3T3 cells.** *A*, the human *BRIL* promoter contains an element between −191 and −204 matching the GLI consensus binding site (*top*, core binding site *highlighted*). The WT and mutant (having a 2-base substitution within the GLI core, *lowercase* at *top*) human −1434 bp promoter Luc constructs (100 ng) were co-transfected in MC3T3 cells with 300 ng of plasmids encoding GFP, GLI1, GLI2, or GLI3. 42 h post-transfection, Luc activity was measured, and results are presented as -fold increase relative to GFP. *Values above bars* represent -fold increases. *B*, the human −1434 bp promoter Luc construct (100 ng) was co-transfected in MC3T3 cells with increasing amounts of plasmid encoding GLI2 (*open symbols*) or with 300 ng of Sp1 (*closed squares*). Luc activity was measured 15, 25, and 42 h post-transfection and expressed as -fold increase relative to a co-transfection with GFP. *C*, MC3T3 cells were co-transfected with the human −1434 bp promoter Luc construct (100 ng) with 150 ng each of GFP or GLI2, in combination with OSX, Sp1, or TCF1, and Luc activity was recorded after 25 h. *D*, real-time quantitative PCR analysis of endogenous *Bril* expression 25 h post-transfection with plasmids encoding GFP, GLI2, or Sp1. Values are normalized to *β-actin* and expressed as $2^{-\Delta}C_t$ relative to the GFP control. Results shown are mean ± S.E. (*error bars*) ($n = 3$–5).

assessed by RT-qPCR in hind limbs at embryonic stages E15.5 and E17.5. As expected, KO mice had almost no detectable *Gli2* expression using a Taqman probe specific for exons 12 and 13 (past the deleted exons 7 and 8) as compared with WT littermates (Fig. 10*A*, *left*). *Bril* expression was decreased 5- and 2.4-fold at E15.5 and E17.5, respectively (Fig. 10*A*, *right*). Tissue sections of tibiae at E17.5 indicated a prominent developmental delay in the KO compared with WT, because they were about 25% shorter with almost no signs of bone formation at the mid-shaft (Fig. 10*B*, *asterisks*). Immunolabeling at E17.5 indicated a considerable reduction in the domain of cells expressing BRIL in the KO compared with the WT (Fig. 10*B*, *bracket*). In the WT mouse, BRIL labeling was observed on osteoblasts at the forming bony collar (Fig. 10*B*, *arrows*), in the primary ossification center (Fig. 10*B*, *asterisks*), and in the perichondrium adjacent to the layers of prehyperthrophic and hyperthrophic chondrocytes (Fig. 10*B*, *arrowheads*). In those areas of BRIL labeling, however, the intensity of the signal did not appear qualitatively reduced. BRIL staining of calvarial osteoblasts did not reveal a significant difference between the WT and the KO (Fig. 10*C*).

Bril Gene Transcription Is Coupled to CpG Demethylation of the Promoter—To explore an epigenetic link to *Bril* gene activation, we examined the CpG methylation status in non-expressing (control) *versus* expressing (PMP-treated) MC3T3 cells. Genomic DNA was isolated from MC3T3 cells 3 days after differentiation in the absence or presence of 1 μM PMP, a time at which endogenous *Bril* is either "off" or "on," respectively (Figs. 8 and 9). Genomic DNA was treated with bisulfite, a chemical that converts all Cs to Ts, unless they are methylated at CpG sites. A 408-bp segment of the mouse *Bril* gene covering −240 to +166 relative to the ATG, contains 12 CpG dinucleotides that are susceptible to be methylated (Fig. 11*A*). Two different primer pairs (F3-R3 and F4-R4) were used to amplify two fragments of 172 and 250 bp, overlapping by 14 bp (Fig. 11*A*). In total, 72 independent clones were sequenced (Fig. 11*B*). In control cells (Fig. 11*B*, *top*), all CpG sites were methylated except for 13 (*filled squares*), representing only 12 independent clones out of 36. In contrast, PMP-treated cells had extensive demethylated CpG, at sites upstream of the ATG (Fig. 11*B*, *bottom*), with six clones being fully demethylated. In non-expressing HEK293 cells, the human *BRIL* gene promoter contains a *bona fide* CpG island, and all CpGs were found to be methylated (data not shown). To test the functional relevance of CpG methylation, the human −1434 bp promoter-Luc plasmid was treated or not *in vitro* with the CpG methyltransferase enzyme M.SssI. Confirming the completeness of the methylation reaction, purified methylated plasmid became resistant to

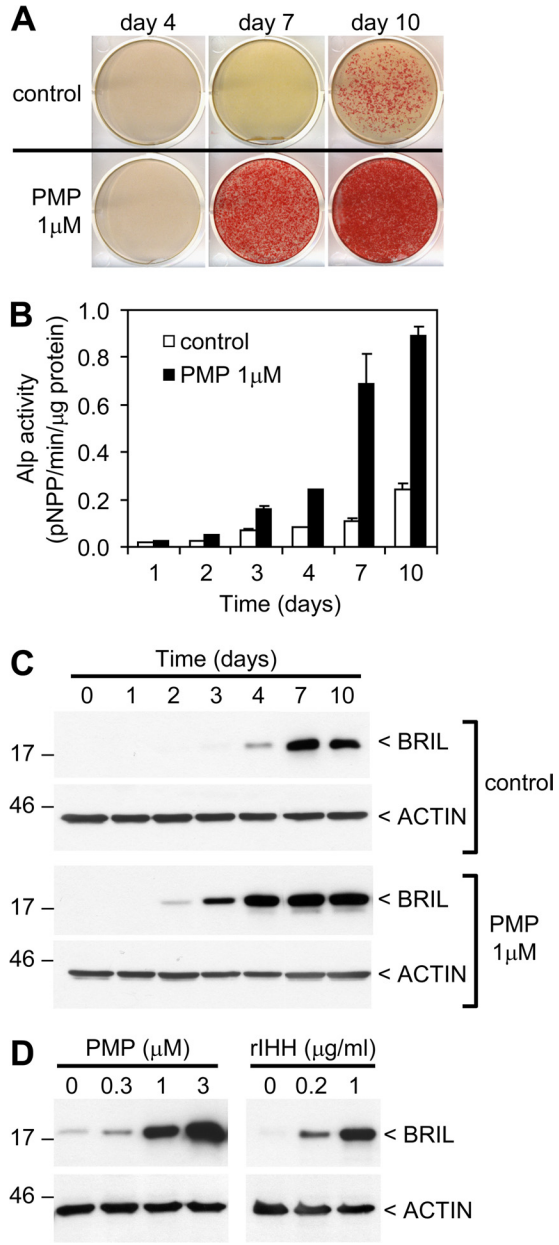

FIGURE 8. **Agonists of the hedgehog pathway increase *Bril* expression in MC3T3 and promote differentiation and mineralization.** Confluent MC3T3 cells (referred to as day 0) were cultured for up to 10 days in differentiation medium in the absence or presence of 1 μM PMP. Control cultures received an equivalent concentration of DMSO (0.05% final). Cells were collected at different time points for analysis of mineral deposition by alizarin red staining (*A*), Alp activity (*B*), and Western blotting for BRIL protein (*C* and *D*). *D*, Western blotting analysis of BRIL in MC3T3 cells cultured from day 0 to 4 with increasing concentrations of PMP (*left*) or rIHH (*right*). Molecular masses are indicated at the *left*. Blots were reprobed for ACTIN as loading controls. Shown are representative results of three independent cultures. *Error bars*, S.E.

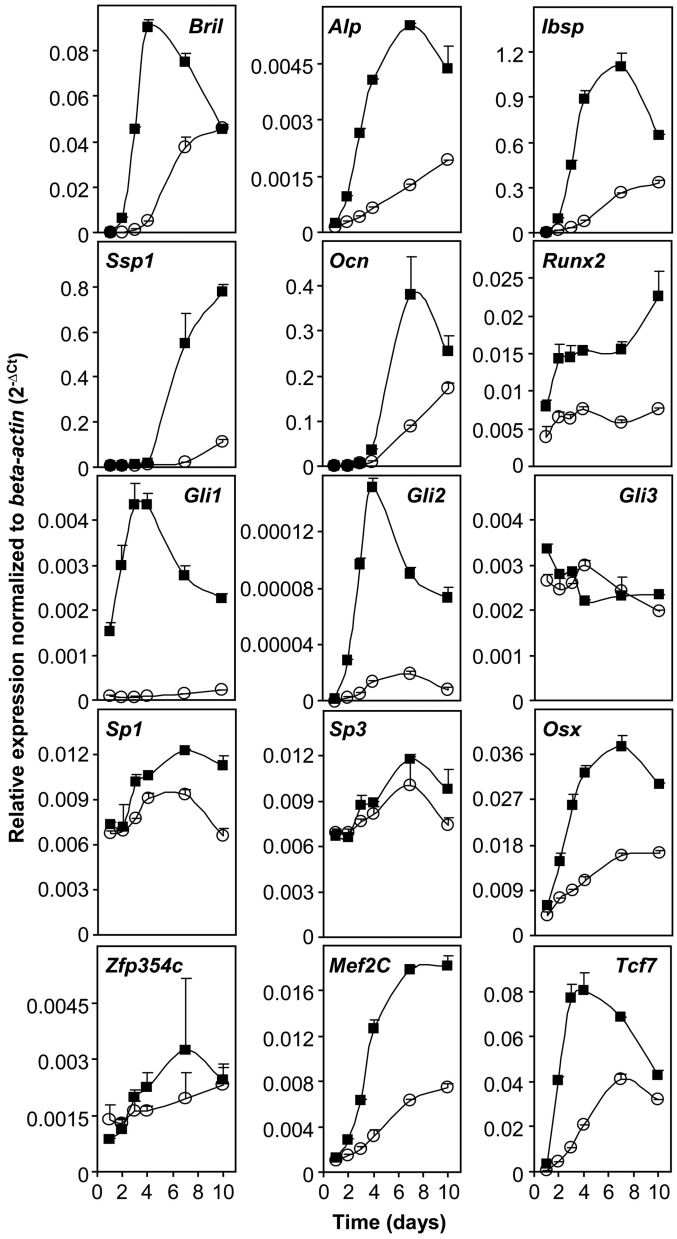

FIGURE 9. **Monitoring of gene expression by qPCR in control and PMP-treated MC3T3 cells.** Differentiating MC3T3 cells were grown in the absence (○) or presence (■) of 1 μM PMP for up to 10 days. Total RNA was extracted after 1, 2, 3, 4, 7, and 10 days and used for RT-qPCR with selected Taqman probes. Values were computed using the threshold cycle method after normalization to *18S* and expressed as $2^{-\Delta}C_t$. Shown are representative results of three independent cultures. *Error bars*, S.E.

restriction at CCGG sites by HpaII (Fig. 11*C*). When assayed by co-transfection in HEK293 cells, both the base-line and Sp1-induced activities of the methylated promoter were reduced down to less than 10% (Fig. 11*D*).

DISCUSSION

Starting from an *in silico* analysis of the conserved *Bril* sequences in rats, mice, and humans, it became obvious that many different elements located within the proximal promoters could contribute to its regulation. We found that the most proximal sequence contained within 250 bp was highly active in the three species after transfection in UMR106 osteosarcoma cells. The activity of the promoter was found to be dependent on the presence of the proximal TATA box (38) located just upstream of the transcriptional start sites. The presence of four canonical binding sites (GC-boxes) (39, 40) for the Sp family bound the specificity proteins Sp1 and Sp3 and contributed to a similar extent to induction of the human, rat, and mouse promoters. In the case of Sp3, several isoforms can be produced from a single transcript (41), and the short forms have been shown to have repressive effects (42, 43). Depending on the

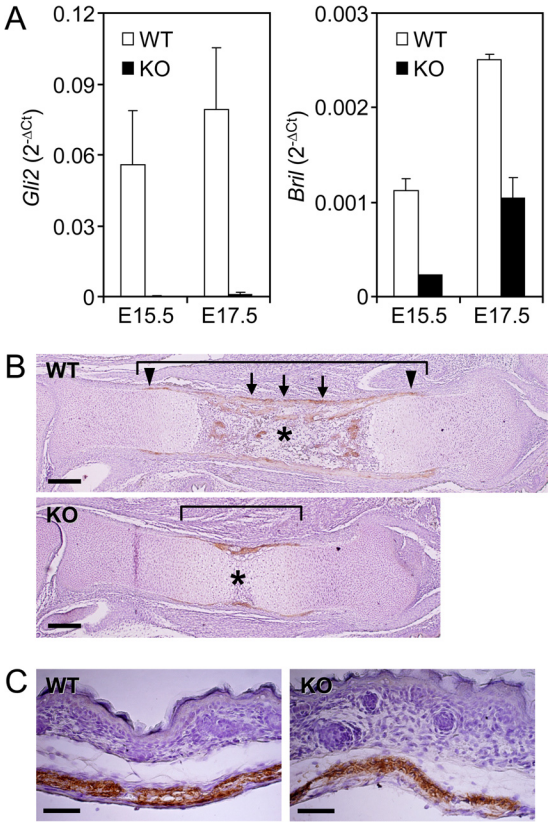

FIGURE 10. **Expression levels and localization of BRIL in embryonic *Gli2* knock-out mice.** *Gli2* heterozygote mice were mated, and embryos were collected at E15.5 and E17.5. *A*, total RNA was extracted from hind limbs of *Gli2* KO ($n = 3$) and WT ($n = 4$) littermates, and RT-qPCR was performed to determine gene expression levels for *Gli2* and *Bril*. Values are normalized to *β-actin* and expressed as $2^{-\Delta}C_t$. Immunohistochemical detection of BRIL at E17.5 on tibia (*B*) and calvaria (*C*) of WT and KO mice is shown. Sections were counterstained with hematoxylin. In *B* and *C*, *bars* indicate 200 and 100 μm, respectively. *Brackets* indicate domain of BRIL immunolabeling; *asterisks* indicate primary ossification center; *arrows* point to bone collar; *arrowheads* show perichondrial osteoblasts. *Error bars*, S.E.

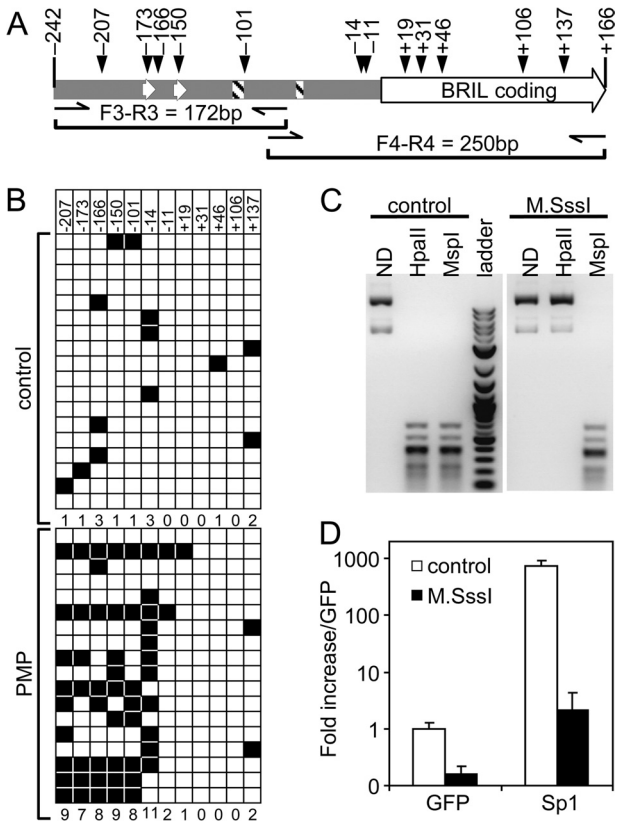

FIGURE 11. **Activation of the *Bril* gene is correlated with extensive CpG demethylation in MC3T3 cells after PMP treatment.** *A*, schematic representation of the mouse *Bril* gene with CpG dinucleotides represented by *black arrows*. The *numbering* is relative to the ATG translation site. The *hatched boxes* and *white arrows* represent the putative TATA boxes and Sp1 sites, respectively. Genomic DNA was isolated from MC3T3 on day 3 after differentiation in the absence (control) or presence of PMP 1 μM. Genomic DNA was treated with bisulfite and amplified using primer pairs F3-R3 and F4-R4. Products of 172 and 250 bp were cloned and sequenced. *B*, results of sequencing, where each *row* represents sequence from a single clone. *Filled squares* indicate the presence of a demethylated CpG site, and *open squares* indicate a methylated site. *C*, the −1434 bp promoter Luc plasmid was treated or not with M.SssI methylase *in vitro* and digested with HpaII, which becomes resistant to cleavage upon methylation (*ND*, non digested). *D*, the control and methylated human −1434 bp promoter plasmids were co-transfected into HEK293 cells with either GFP or Sp1. Luc activity was measured 42 h later and normalized to the control GFP values. *Error bars*, S.E.

promoter context, Sp3 can either synergize or repress Sp1-mediated transcription (44, 45). However, the long forms of Sp3 were found to be equally effective as Sp1 at activating the *Bril* promoters, whereas the short form had no transacting properties on its own. Furthermore, co-transfection studies indicated that the human *BRIL* promoter responded in a synergistic fashion to Sp1 alone or in combination with all three Sp3 isoforms. The nature of the response is in line with the known transactivating properties of Sp1, which can be increased through direct or indirect interaction with a plethora of molecules, including itself (44, 45). Sp1 oligomers can thus synergistically transactivate at promoters containing multiple copies of its DNA binding element, through cooperative DNA binding, which was also observed on the human *BRIL* promoter. Sp1 and Sp3 are considered rather ubiquitous transcription factors, yet they have been found to contribute to the tissue-specific activation of a number of genes expressed in bones, such as *Runx2*, *Osx*, *Alp*, *Col11a2*, *Rankl*, and *Ocn* (46–51). Consistent with this, we have shown that the levels of *Sp1* and *Sp3* in differentiating MC3T3 remained relatively constant. Although they are not considered to be controlling major pathways specific for bone development and formation, Sp3 null mice do show bone and tooth formation defects (52, 53). On the other hand, the OSX transcription factor, a member of the Sp protein family called Sp7, represented a more probable candidate regulator of *Bril*. OSX is known to act downstream of RUNX2 in osteoblastic differentiation, and both factors are considered as master regulators of osteoblastogenesis (54, 55). Through binding GC-rich elements, OSX orchestrates expression of many genes involved in bone formation (56). Despite the presence of several functionally active Sp1 sites, OSX turned out to be totally inactive in HEK293 cells and only marginally effective in MC3T3 osteoblasts. We showed, however, that OSX was able to synergistically activate *BRIL* in the presence of Sp1, suggesting that they could have mutually interacted or facilitated binding to their cognate element. In support of this possibility, a study similar to ours looking at the regulation of the rat *Ocn* promoter found that OSX activity was dependent on the requirement of Sp1 (57). Although binding of OSX was found to occur at a CCAAT box just upstream of the canonical Sp1 binding site, co-immu-

noprecipitation indicated a physical interaction between OSX and Sp1 (57). Such a mechanism could be operative at the *Bril* promoter. Considering the complex mode of OSX function, it is also possible that conditions inherent to our experimental setup may have contributed in part to the weak response. For instance, OSX transcriptional properties were shown to be modulated, positively and negatively, by interaction with the co-activator NFATc1 (58) and the lysine histone demethylase NO66 (59) and further modulated by phosphorylation (56). The same could apply to RUNX2, which was inactive on *Bril*, even when tested in the context of the 3′-conserved region that contained two canonical RUNX2 binding elements. *Bril* was previously reported to be up-regulated by overexpression of RUNX2 in limb bud cultures to the same extent as *Osx*, *Phex*, *Ocn*, and *Ibsp* (60). In that same study, *Bril* was found to be down-regulated in the limbs of *Osx* knock-out mice, but the reported effects may have been indirect, due to either increased or decreased differentiation of osteoblasts.

One of the most frequent putative binding sites found on the *Bril* promoter region (CCAC) was that of the ZFP354C transcription factor. Our results showed that ZFP354C reduced the basal level of the *BRIL* promoter activity and inhibited the Sp1-mediated induction, even when combined at ratios of as low as 1:6, and totally abrogated the Sp1 effect at 1:1. ZFP354C is a KRAB domain protein containing 11 C2H2-type zinc fingers. ZFP354C is expressed in many different tissues, including bone (61, 62). Like the other family members ZFP354A and ZFP354B (63), ZFP354C was shown to act as a transcriptional repressor (64). The core consensus DNA binding element of ZFP354C resembles that of the RUNX2 binding site (62, 65). ZFP354C was reported to antagonize RUNX2-mediated transcriptional activation on a multimerized RUNX2 element (62). Functionally, very little is known about ZFP354C, yet it has been suggested to act as a negative regulator of osteogenesis, because its overexpression in C3H10T1/2 reduced BMP4-induced osteogenic differentiation and expression of *Alp* (62). However, opposite effects were observed in stably expressing rat stromal bone marrow cells, with ZFP354C promoting differentiation and mineralization (61). Although we have not directly investigated the mechanisms involved, we speculate that ZFP354C could bind directly to the putative CCAC elements within the *BRIL* proximal promoter. In fact, there are a total of 10 CCAC elements within the human *BRIL* promoter, at least two overlapping with the functional Sp1-2 and Sp1-3 sites. Binding of ZFP354C could impede subsequent binding of other factors. Although the levels of ZFP354C did not change appreciably during MC3T3 cell differentiation, we found that relative expression of *Zfp354c* was 60 times greater in non-expressing HEK293 than in expressing UMR106 and MC3T3 cells (data not shown). Our results suggest that a delicate balance between activators and repressors would contribute to establishing *Bril* expression.

Another mode of regulation identified here that intersected at least in part with the Sp1 regulation is the methylation status of the *Bril* promoter. The *Bril* gene promoters are all GC-rich (up to 70% on 50–70-bp stretches) and contain several CpG dinucleotides covering the promoter and coding region of exon 1. Furthermore, the human *BRIL* is predicted to contain a *bona fide* CpG island. CpG islands clustered at most gene promoters are usually kept unmethylated, thus creating a transcriptional permissive state (66). Reciprocally, methylation of CpG dinucleotides is often associated with silent chromatin, being refractory to transcriptional initiation (66). Usually, promoters having CpG islands are relatively nucleosome-deficient, allowing greater accessibility of the underlying DNA to transcriptional regulators. However, the *BRIL* gene was found to be fully methylated in non-expressing HEK293 cells and also in permissive but non-differentiated MC3T3 cells. Accelerating differentiation of MC3T3 cells with PMP was associated with a considerable demethylation of CpG sites in the promoter and 5′-UTR region but not over the coding region of exon 1. Consistent with the negative effects of promoter methylation, treatment of the human promoter with CpG methylase *in vitro* resulted in a considerable reduction of its base-line activity and a total abrogation of responsiveness to Sp1. Studies looking at other gene promoters have also reported the repressive effect of CpG methylation on Sp1/Sp3-mediated gene activation (67–69). Thus, in non-expressing cells, methylation of the *Bril* promoter region would restrict accessibility to activators. Demethylation alone did not appear to be sufficient to activate *Bril* expression, because treatment with 5-aza-2′-deoxycytidine, a drug that prevents DNA methylation, did not activate *Bril* in HEK293 and NIH3T3 cells (data not shown). The exact sequence of events, however, that triggers demethylation of the *Bril* promoter is unclear, but could involve modulated expression of different molecules having such activities. In a recent study (70), DMSO treatment of MC3T3 cells was found to globally reduce CpG methylation. DMSO was found to down-regulate gene expression and protein levels of methylation prone molecules (DNMT1, DNMT3, and HELLS) and to up-regulate enzymes (TET and GADD45) sequentially involved in the conversion of methylcytosine to 5-hydroxymethylcytosine, an intermediate to unmethylated CpG. Although *Dlx5* and *Fas* genes and promoter methylation were clearly affected by DMSO treatment, a global gene expression profile monitored by microarrays did not identify *Bril* as being changed after 5 days of culture (70). Another study previously implicated the MEF2C transcription factor in the DMSO-induced MC3T3 differentiation and mineralization (71). In that study, microarray analysis of DMSO-treated MC3T3 cells identified *Bril* as being significantly up-regulated 1.6-fold and down-regulated 4.2-fold after knockdown of *Mef2c*. Our expression data in MC3T3 confirmed that MEF2C was increased along the differentiation program and was further enhanced by PMP treatment. MEF2C was a strong inducer of the *Bril* promoter activity (>25-fold) in HEK293 cells but only weakly activated in MC3T3 cells (~3-fold) (supplemental Fig. 1). We cannot formally rule out the possibility that MEF2C could have contributed to *Bril* expression, independent on the effects of DMSO because the concentration used under our current experimental conditions (0.05%) was 3 times less than the minimal effective concentration that elicited a response in the preceding study. Regulation of gene transcription through DNA methylation is not unique to *Bril*, because this type of epigenetic event has been detailed previously for a number of bone-related genes, *Dlx5* (72), *Alp* (73), *Sost* (74), and *Osx* (75).

Last, we have provided several lines of evidence indicating that the hedgehog pathway participates in the regulation of *Bril* expression. A high affinity binding site for GLI (36, 37) was found in the proximal promoter across species. We found that this element was essential to mediate strong transactivation of the *BRIL* promoter to GLI2 and much less to mediate transactivation to GLI1 and GLI3. GLI2 was also found to be much more potent than Sp1, activating *BRIL* at maximal levels very early after transfection and requiring much smaller quantities of plasmid DNA. Furthermore, co-transfection experiments of GLI2 with Sp1 or OSX indicated a synergistic mode of activation at the *BRIL* promoter. Sp1 is known to interact with a vast number of different proteins (44, 45), but an interaction with GLI2 has not been reported previously, and future work is required to reveal whether they can physically interact. The up-regulation of the endogenous *Bril* after overexpression of GLI2 in MC3T3 is compelling evidence of a direct effect, at least *in vitro*. This is also supported by the activation of the *Bril* gene after treatment of MC3T3 with agonists of the hedgehog pathway, either with PMP or rIHH in a time- and concentration-dependent manner. Hedgehog signaling is initiated by binding PTCH, thus relieving its inhibitory effect on SMO, the primary effector of the signaling cascade. Through a series of cytoplasmic events, SMO controls the proteolytic processing, activity, and subcellular localization of GLI proteins that regulate downstream gene targets (76–78). PMP is a small molecule agonist of SMO that was reported to promote osteoblastic differentiation using ALP activity as a readout (79–81). The positive effects of PMP and rIHH on BRIL expression indicated that the PTCH-SMO-GLI pathway is operative in our system. IHH, a soluble factor secreted by prehyperthrophic chondrocytes of the growth plate, is essential for osteoblast differentiation *in vivo*, where it signals to the perichondrial cells adjacent to hyperthrophic chondrocytes of the bone collar region to induce their differentiation into fully mature mineralizing osteoblasts (78, 82–85). In fact, the expression and localization of BRIL in embryonic long bones that we have previously reported (5) and shown here (Fig. 10) exactly coincides with the domain of osteoblasts responsive to IHH cues. Last, PMP treatment not only increased Alp activity but also dramatically accelerated and increased the extent of mineralization, suggesting that the effects may have been mediated in part by increased differentiation. In support of this, our gene expression profiling indicated that PMP favored increased expression of several gene markers (*Ibsp*, *Alp*, *Osx*, *Gli2*, and *Tcf7*) of osteoblastic differentiation with a kinetics very similar to that of *Bril*. The observation that *Runx2* levels were doubled is also suggestive of increased and/or accelerated differentiation. Robust increases in *Gli1* were observed only after 24 h of PMP treatment. Because GLI1 is considered a downstream target of *Gli2*, this would suggest a feed forward mechanism driven by endogenous GLI2 in MC3T3. Possible mechanisms leading to increased differentiation and mineralization after hedgehog stimulation have been proposed to involve *Bmp2* in C2C12 and 2T3 cells (78), *Osx* in MC3T3 (86), and *Runx2* in C3HT101/2 (87).

To determine whether *Bril* is a direct target of GLI2 *in vivo*, we studied its expression in *Gli2* mutant mice in which the DNA binding function of GLI2 is disrupted after deletion of zinc fingers 3–5 (34). These mice die in late gestation and perinatally due to a number of tissue defects and display skeletal growth retardation due to improper development of the growth plate during endochondral ossification (33). Congruent with the possibility of *Bril* being directly modulated by the hedgehog pathway *in vivo*, we found that expression levels of *Bril* in hind limbs at E15.5 and E17.5 were reduced to less than half. As expected based on our earlier work (5), immunohistochemical localization of BRIL in the tibiae of wild type mice confirmed that it is restricted to the forming perichondrium adjacent to the growth plate, to the developing bony collar, and to primary spongiosa. In contrast, the surface area containing cells immunoreactive for BRIL was reduced in the tibia of *Gli2* knock-out mice, with an almost total absence of BRIL in the forming trabeculae at the midshaft region. However, the intensity of the signal was qualitatively similar in *Gli2* knock-out relative to wild type mice, especially in differentiating osteoblasts along the bone collar. These results would suggest that other factors may have compensated for the lack of GLI2 and contributed to *Bril* expression. The small yet significant stimulation of the *BRIL* promoter by GLI1 would support such a hypothesis. Studies aiming to understand the regulation of osteogenesis by GLI family members have revealed a complex scenario, pointing to the overall effects of hedgehog on osteoblasts being highly dependent on the timing, location, and strength of signaling. All three *Gli* genes are expressed in overlapping subsets of cells in the developing long bones, including osteoblasts (88). It is not entirely clear whether the GLI proteins can functionally substitute for each other or work in combination, but certainly the activator function of GLI2 is necessary for osteoblast differentiation (89). At the same time, the primary repressor function of GLI3 needs to be alleviated for proper osteogenesis, because it directly interfered with DNA binding activity of RUNX2 at osteogenic target genes (90). Although the activating function of GLI1 was found to be dispensable *in vivo* for mouse development (91), recent evidence has indicated that it is also important for endochondral ossification (24).

In conclusion, we have provided the first detailed analysis of the transcriptional regulation of the *Bril* gene. Commonalities were found between the three species studied, suggesting that these are genuine pathways likely to control *Bril* transcription. Unexpectedly, different transcription factors were identified that either activated or repressed transcription, some of them acting in a coordinated and synergistic manner. The contribution of potential distal enhancers to *Bril* expression is another possibility that we have not yet explored. We also uncovered an epigenetic mode of regulation, through CpG demethylation of the *Bril* promoter region, triggering a transcriptionally permissible state. Altogether, these data provide basic mechanisms controlling the osteoblast-specific nature of *Bril*, an important player in bone physiology.

Acknowledgments—We thank Lisa Lamplugh and Dr. Antonio Nanci for help with processing of tissue sections and Dr. Peter J. Roughley for helpful comments on the manuscript.

REFERENCES

1. Moffatt, P., Salois, P., Gaumond, M. H., St-Amant, N., Godin, E., and Lanctôt, C. (2002) Engineered viruses to select genes encoding secreted and membrane-bound proteins in mammalian cells. *Nucleic Acids Res.* **30,** 4285–4294
2. Siegrist, F., Ebeling, M., and Certa, U. (2011) The small interferon-induced transmembrane genes and proteins. *J. Interferon Cytokine Res.* **31,** 183–197
3. Hickford, D., Frankenberg, S., Shaw, G., and Renfree, M. B. (2012) Evolution of vertebrate interferon inducible transmembrane proteins. *BMC. Genomics* **13,** 155
4. Sällman Almén, M., Bringeland, N., Fredriksson, R., and Schiöth, H. B. (2012) The dispanins. A novel gene family of ancient origin that contains 14 human members. *PLoS One* **7,** e31961
5. Moffatt, P., Gaumond, M. H., Salois, P., Sellin, K., Bessette, M. C., Godin, E., de Oliveira, P. T., Atkins, G. J., Nanci, A., and Thomas, G. (2008) Bril. A novel bone-specific modulator of mineralization. *J. Bone Miner. Res.* **23,** 1497–1508
6. Brass, A. L., Huang, I. C., Benita, Y., John, S. P., Krishnan, M. N., Feeley, E. M., Ryan, B. J., Weyer, J. L., van der Weyden, L., Fikrig, E., Adams, D. J., Xavier, R. J., Farzan, M., and Elledge, S. J. (2009) The IFITM proteins mediate cellular resistance to influenza A H1N1 virus, West Nile virus, and dengue virus. *Cell* **139,** 1243–1254
7. Yount, J. S., Moltedo, B., Yang, Y. Y., Charron, G., Moran, T. M., López, C. B., and Hang, H. C. (2010) Palmitoylome profiling reveals *S*-palmitoylation-dependent antiviral activity of IFITM3. *Nat. Chem. Biol.* **6,** 610–614
8. Jia, R., Pan, Q., Ding, S., Rong, L., Liu, S. L., Geng, Y., Qiao, W., and Liang, C. (2012) The N-terminal region of IFITM3 modulates its antiviral activity through regulating IFITM3 cellular localization. *J. Virol.* **86,** 13697–13707
9. Yount, J. S., Karssemeijer, R. A., and Hang, H. C. (2012) *S*-Palmitoylation and ubiquitination differentially regulate interferon-induced transmembrane protein 3 (IFITM3)-mediated resistance to influenza virus. *J. Biol. Chem.* **287,** 19631–19641
10. Lewin, A. R., Reid, L. E., McMahon, M., Stark, G. R., and Kerr, I. M. (1991) Molecular analysis of a human interferon-inducible gene family. *Eur. J. Biochem.* **199,** 417–423
11. Bailey, C. C., Huang, I. C., Kam, C., and Farzan, M. (2012) Ifitm3 limits the severity of acute influenza in mice. *PLoS Pathog.* **8,** e1002909
12. Cho, T. J., Lee, K. E., Lee, S. K., Song, S. J., Kim, K. J., Jeon, D., Lee, G., Kim, H. N., Lee, H. R., Eom, H. H., Lee, Z. H., Kim, O. H., Park, W. Y., Park, S. S., Ikegawa, S., Yoo, W. J., Choi, I. H., and Kim, J. W. (2012) A single recurrent mutation in the 5′-UTR of IFITM5 causes osteogenesis imperfecta type V. *Am. J. Hum. Genet.* **91,** 343–348
13. Hanagata, N., Takemura, T., Monkawa, A., Ikoma, T., and Tanaka, J. (2007) Phenotype and gene expression pattern of osteoblast-like cells cultured on polystyrene and hydroxyapatite with pre-adsorbed type-I collagen. *J. Biomed. Mater. Res. A* **83,** 362–371
14. Rigden, D. J., Woodhead, D. D., Wong, P. W., and Galperin, M. Y. (2011) New structural and functional contexts of the Dx[DN]xDG linear motif. Insights into evolution of calcium-binding proteins. *PLoS One* **6,** e21507
15. Hanagata, N., and Li, X. (2011) Osteoblast-enriched membrane protein IFITM5 regulates the association of CD9 with an FKBP11-CD81-FPRP complex and stimulates expression of interferon-induced genes. *Biochem. Biophys. Res. Commun.* **409,** 378–384
16. Hanagata, N., Li, X., Morita, H., Takemura, T., Li, J., and Minowa, T. (2011) Characterization of the osteoblast-specific transmembrane protein IFITM5 and analysis of IFITM5-deficient mice. *J. Bone Miner. Metab.* **29,** 279–290
17. Lange, U. C., Adams, D. J., Lee, C., Barton, S., Schneider, R., Bradley, A., and Surani, M. A. (2008) Normal germ line establishment in mice carrying a deletion of the Ifitm/Fragilis gene family cluster. *Mol. Cell Biol.* **28,** 4688–4696
18. Feeley, E. M., Sims, J. S., John, S. P., Chin, C. R., Pertel, T., Chen, L. M., Gaiha, G. D., Ryan, B. J., Donis, R. O., Elledge, S. J., and Brass, A. L. (2011) IFITM3 inhibits influenza A virus infection by preventing cytosolic entry. *PLoS Pathog.* **7,** e1002337
19. Huang, I. C., Bailey, C. C., Weyer, J. L., Radoshitzky, S. R., Becker, M. M., Chiang, J. J., Brass, A. L., Ahmed, A. A., Chi, X., Dong, L., Longobardi, L. E., Boltz, D., Kuhn, J. H., Elledge, S. J., Bavari, S., Denison, M. R., Choe, H., and Farzan, M. (2011) Distinct patterns of IFITM-mediated restriction of filoviruses, SARS coronavirus, and influenza A virus. *PLoS Pathog.* **7,** e1001258
20. Jiang, D., Weidner, J. M., Qing, M., Pan, X. B., Guo, H., Xu, C., Zhang, X., Birk, A., Chang, J., Shi, P. Y., Block, T. M., and Guo, J. T. (2010) Identification of five interferon-induced cellular proteins that inhibit West Nile virus and dengue virus infections. *J. Virol.* **84,** 8332–8341
21. Lu, J., Pan, Q., Rong, L., He, W., Liu, S. L., and Liang, C. (2011) The IFITM proteins inhibit HIV-1 infection. *J. Virol.* **85,** 2126–2137
22. Raychoudhuri, A., Shrivastava, S., Steele, R., Kim, H., Ray, R., and Ray, R. B. (2011) ISG56 and IFITM1 proteins inhibit hepatitis C virus replication. *J. Virol.* **85,** 12881–12889
23. Weidner, J. M., Jiang, D., Pan, X. B., Chang, J., Block, T. M., and Guo, J. T. (2010) Interferon-induced cell membrane proteins, IFITM3 and tetherin, inhibit vesicular stomatitis virus infection via distinct mechanisms. *J. Virol.* **84,** 12646–12657
24. Hojo, H., Ohba, S., Yano, F., Saito, T., Ikeda, T., Nakajima, K., Komiyama, Y., Nakagata, N., Suzuki, K., Takato, T., Kawaguchi, H., and Chung, U. I. (2012) Gli1 protein participates in hedgehog-mediated specification of osteoblast lineage during endochondral ossification. *J. Biol. Chem.* **287,** 17860–17869
25. Semler, O., Garbes, L., Keupp, K., Swan, D., Zimmermann, K., Becker, J., Iden, S., Wirth, B., Eysel, P., Koerber, F., Schoenau, E., Bohlander, S. K., Wollnik, B., and Netzer, C. (2012) A mutation in the 5′-UTR of IFITM5 creates an in-frame start codon and causes autosomal-dominant osteogenesis imperfecta type V with hyperplastic callus. *Am. J. Hum. Genet.* **91,** 349–357
26. Glorieux, F. H., Rauch, F., Plotkin, H., Ward, L., Travers, R., Roughley, P., Lalic, L., Glorieux, D. F., Fassier, F., and Bishop, N. J. (2000) Type V osteogenesis imperfecta. A new form of brittle bone disease. *J. Bone Miner. Res.* **15,** 1650–1658
27. Rauch, F., Moffatt, P., Cheung, M., Roughley, P., Lalic, L., Lund, A. M., Ramirez, N., Fahiminiya, S., Majewski, J., and Glorieux, F. H. (2013) Osteogenesis imperfecta type V. Marked phenotypic variability despite the presence of the IFITM5 c.-14C→T mutation in all patients. *J Med. Genet.* **50,** 21–24
28. Schmittgen, T. D., and Livak, K. J. (2008) Analyzing real-time PCR data by the comparative C_T method. *Nat. Protoc.* **3,** 1101–1108
29. Moffatt, P., Salois, P., St-Amant, N., Gaumond, M. H., and Lanctôt, C. (2004) Identification of a conserved cluster of skin-specific genes encoding secreted proteins. *Gene* **334,** 123–131
30. Müller, M. M., Schreiber, E., Schaffner, W., and Matthias, P. (1989) Rapid test for *in vivo* stability and DNA binding of mutated octamer binding proteins with "mini-extracts" prepared from transfected cells. *Nucleic Acids Res.* **17,** 6420
31. Faraonio, R., Moffatt, P., Larochelle, O., Schipper, H. M., S-Arnaud, R., and Séguin, C. (2000) Characterization of cis-acting elements in the promoter of the mouse metallothionein-3 gene. Activation of gene expression during neuronal differentiation of P19 embryonal carcinoma cells. *Eur. J. Biochem.* **267,** 1743–1753
32. Larochelle, O., Stewart, G., Moffatt, P., Tremblay, V., and Séguin, C. (2001) Characterization of the mouse metal-regulatory-element-binding proteins, metal element protein-1 and metal regulatory transcription factor-1. *Biochem. J* **353,** 591–601
33. Miao, D., Liu, H., Plut, P., Niu, M., Huo, R., Goltzman, D., and Henderson, J. E. (2004) Impaired endochondral bone development and osteopenia in Gli2-deficient mice. *Exp. Cell Res.* **294,** 210–222
34. Mo, R., Freer, A. M., Zinyk, D. L., Crackower, M. A., Michaud, J., Heng, H. H., Chik, K. W., Shi, X. M., Tsui, L. C., Cheng, S. H., Joyner, A. L., and Hui, C. (1997) Specific and redundant functions of Gli2 and Gli3 zinc finger genes in skeletal patterning and development. *Development* **124,** 113–123
35. Li, L. C., and Dahiya, R. (2002) MethPrimer: designing primers for methylation PCRs. *Bioinformatics* **18,** 1427–1431
36. Kinzler, K. W., and Vogelstein, B. (1990) The GLI gene encodes a nuclear

protein which binds specific sequences in the human genome. *Mol. Cell Biol.* **10,** 634–642
37. Winklmayr, M., Schmid, C., Laner-Plamberger, S., Kaser, A., Aberger, F., Eichberger, T., and Frischauf, A. M. (2010) Non-consensus GLI binding sites in hedgehog target gene regulation. *BMC Mol. Biol.* **11,** 2
38. Smale, S. T., and Kadonaga, J. T. (2003) The RNA polymerase II core promoter. *Annu. Rev. Biochem.* **72,** 449–479
39. Bucher, P. (1990) Weight matrix descriptions of four eukaryotic RNA polymerase II promoter elements derived from 502 unrelated promoter sequences. *J. Mol. Biol.* **212,** 563–578
40. Letovsky, J., and Dynan, W. S. (1989) Measurement of the binding of transcription factor Sp1 to a single GC box recognition sequence. *Nucleic Acids Res.* **17,** 2639–2653
41. Sapetschnig, A., Koch, F., Rischitor, G., Mennenga, T., and Suske, G. (2004) Complexity of translationally controlled transcription factor Sp3 isoform expression. *J. Biol. Chem.* **279,** 42095–42105
42. Hagen, G., Müller, S., Beato, M., and Suske, G. (1994) Sp1-mediated transcriptional activation is repressed by Sp3. *EMBO J.* **13,** 3843–3851
43. Kennett, S. B., Udvadia, A. J., and Horowitz, J. M. (1997) Sp3 encodes multiple proteins that differ in their capacity to stimulate or repress transcription. *Nucleic Acids Res.* **25,** 3110–3117
44. Li, L., He, S., Sun, J. M., and Davie, J. R. (2004) Gene regulation by Sp1 and Sp3. *Biochem. Cell Biol.* **82,** 460–471
45. Wierstra, I. (2008) Sp1. Emerging roles. Beyond constitutive activation of TATA-less housekeeping genes. *Biochem. Biophys. Res. Commun.* **372,** 1–13
46. Goto, T., Matsui, Y., Fernandes, R. J., Hanson, D. A., Kubo, T., Yukata, K., Michigami, T., Komori, T., Fujita, T., Yang, L., Eyre, D. R., and Yasui, N. (2006) Sp1 family of transcription factors regulates the human alpha2 (XI) collagen gene (COL11A2) in Saos-2 osteoblastic cells. *J Bone Miner. Res.* **21,** 661–673
47. Le Mée, S., Fromigué, O., and Marie, P. J. (2005) Sp1/Sp3 and the myeloid zinc finger gene MZF1 regulate the human N-cadherin promoter in osteoblasts. *Exp. Cell Res.* **302,** 129–142
48. Liu, J., Yang, H., Liu, W., Cao, X., and Feng, X. (2005) Sp1 and Sp3 regulate the basal transcription of receptor activator of nuclear factor κB ligand gene in osteoblasts and bone marrow stromal cells. *J. Cell Biochem.* **96,** 716–727
49. Stains, J. P., Lecanda, F., Screen, J., Towler, D. A., and Civitelli, R. (2003) Gap junctional communication modulates gene transcription by altering the recruitment of Sp1 and Sp3 to connexin-response elements in osteoblast promoters. *J. Biol. Chem.* **278,** 24377–24387
50. Yusa, N., Watanabe, K., Yoshida, S., Shirafuji, N., Shimomura, S., Tani, K., Asano, S., and Sato, N. (2000) Transcription factor Sp3 activates the liver/bone/kidney-type alkaline phosphatase promoter in hematopoietic cells. *J. Leukoc. Biol.* **68,** 772–777
51. Zhang, Y., Hassan, M. Q., Xie, R. L., Hawse, J. R., Spelsberg, T. C., Montecino, M., Stein, J. L., Lian, J. B., van Wijnen, A. J., and Stein, G. S. (2009) Co-stimulation of the bone-related Runx2 P1 promoter in mesenchymal cells by SP1 and ETS transcription factors at polymorphic purine-rich DNA sequences (Y-repeats). *J. Biol. Chem.* **284,** 3125–3135
52. Bouwman, P., Göllner, H., Elsässer, H. P., Eckhoff, G., Karis, A., Grosveld, F., Philipsen, S., and Suske, G. (2000) Transcription factor Sp3 is essential for post-natal survival and late tooth development. *EMBO J.* **19,** 655–661
53. Göllner, H., Dani, C., Phillips, B., Philipsen, S., and Suske, G. (2001) Impaired ossification in mice lacking the transcription factor Sp3. *Mech. Dev.* **106,** 77–83
54. Nakashima, K., Zhou, X., Kunkel, G., Zhang, Z., Deng, J. M., Behringer, R. R., and de Crombrugghe, B. (2002) The novel zinc finger-containing transcription factor osterix is required for osteoblast differentiation and bone formation. *Cell* **108,** 17–29
55. Ducy, P., Zhang, R., Geoffroy, V., Ridall, A. L., and Karsenty, G. (1997) Osf2/Cbfa1. A transcriptional activator of osteoblast differentiation. *Cell* **89,** 747–754
56. Sinha, K. M., and Zhou, X. (2013) Genetic and molecular control of Osterix in skeletal formation. *J. Cell Biochem.* **114,** 975–984
57. Niger, C., Lima, F., Yoo, D. J., Gupta, R. R., Buo, A. M., Hebert, C., and Stains, J. P. (2011) The transcriptional activity of osterix requires the recruitment of Sp1 to the osteocalcin proximal promoter. *Bone* **49,** 683–692
58. Koga, T., Matsui, Y., Asagiri, M., Kodama, T., de Crombrugghe, B., Nakashima, K., and Takayanagi, H. (2005) NFAT and Osterix cooperatively regulate bone formation. *Nat. Med.* **11,** 880–885
59. Sinha, K. M., Yasuda, H., Coombes, M. M., Dent, S. Y., and de Crombrugghe, B. (2010) Regulation of the osteoblast-specific transcription factor Osterix by NO66, a Jumonji family histone demethylase. *EMBO J.* **29,** 68–79
60. Nishimura, R., Wakabayashi, M., Hata, K., Matsubara, T., Honma, S., Wakisaka, S., Kiyonari, H., Shioi, G., Yamaguchi, A., Tsumaki, N., Akiyama, H., and Yoneda, T. (2012) Osterix regulates calcification and degradation of chondrogenic matrices through matrix metalloproteinase 13 (MMP13) expression in association with transcription factor Runx2 during endochondral ossification. *J. Biol. Chem.* **287,** 33179–33190
61. Jheon, A., Bansal, A. K., Zhu, B., Ganss, B., Cheifetz, S., and Sodek, J. (2009) Characterisation of the constitutive over-expression of AJ18 in a novel rat stromal bone marrow cell line (D8-SBMC). *Arch. Oral Biol.* **54,** 705–716
62. Jheon, A. H., Ganss, B., Cheifetz, S., and Sodek, J. (2001) Characterization of a novel KRAB/C2H2 zinc finger transcription factor involved in bone development. *J. Biol. Chem.* **276,** 18282–18289
63. Urrutia, R. (2003) KRAB-containing zinc-finger repressor proteins. *Genome Biol.* **4,** 231
64. Witzgall, R., O'Leary, E., Leaf, A., Onaldi, D., and Bonventre, J. V. (1994) The Kruppel-associated box-A (KRAB-A) domain of zinc finger proteins mediates transcriptional repression. *Proc. Natl. Acad. Sci. U.S.A.* **91,** 4514–4518
65. Gao, L., Sun, C., Qiu, H. L., Liu, H., Shao, H. J., Wang, J., and Li, W. X. (2004) Cloning and characterization of a novel human zinc finger gene, hKid3, from a C2H2-ZNF enriched human embryonic cDNA library. *Biochem. Biophys. Res. Commun.* **325,** 1145–1152
66. Deaton, A. M., and Bird, A. (2011) CpG islands and the regulation of transcription. *Genes Dev.* **25,** 1010–1022
67. Aoyama, T., Okamoto, T., Nagayama, S., Nishijo, K., Ishibe, T., Yasura, K., Nakayama, T., Nakamura, T., and Toguchida, J. (2004) Methylation in the core-promoter region of the chondromodulin-I gene determines the cell-specific expression by regulating the binding of transcriptional activator Sp3. *J. Biol. Chem.* **279,** 28789–28797
68. Zelko, I. N., Mueller, M. R., and Folz, R. J. (2010) CpG methylation attenuates Sp1 and Sp3 binding to the human extracellular superoxide dismutase promoter and regulates its cell-specific expression. *Free Radic. Biol. Med.* **48,** 895–904
69. Zhu, W. G., Srinivasan, K., Dai, Z., Duan, W., Druhan, L. J., Ding, H., Yee, L., Villalona-Calero, M. A., Plass, C., and Otterson, G. A. (2003) Methylation of adjacent CpG sites affects Sp1/Sp3 binding and activity in the $p21^{Cip1}$ promoter. *Mol. Cell Biol.* **23,** 4056–4065
70. Thaler, R., Spitzer, S., Karlic, H., Klaushofer, K., and Varga, F. (2012) DMSO is a strong inducer of DNA hydroxymethylation in pre-osteoblastic MC3T3-E1 cells. *Epigenetics* **7,** 635–651
71. Stephens, A. S., Stephens, S. R., Hobbs, C., Hutmacher, D. W., Bacic-Welsh, D., Woodruff, M. A., and Morrison, N. A. (2011) Myocyte enhancer factor 2c, an osteoblast transcription factor identified by dimethyl sulfoxide (DMSO)-enhanced mineralization. *J. Biol. Chem.* **286,** 30071–30086
72. Lee, J. Y., Lee, Y. M., Kim, M. J., Choi, J. Y., Park, E. K., Kim, S. Y., Lee, S. P., Yang, J. S., and Kim, D. S. (2006) Methylation of the mouse DIx5 and Osx gene promoters regulates cell type-specific gene expression. *Mol. Cells* **22,** 182–188
73. Delgado-Calle, J., Sañudo, C., Sánchez-Verde, L., García-Renedo, R. J., Arozamena, J., and Riancho, J. A. (2011) Epigenetic regulation of alkaline phosphatase in human cells of the osteoblastic lineage. *Bone* **49,** 830–838
74. Delgado-Calle, J., Sañudo, C., Bolado, A., Fernández, A. F., Arozamena, J., Pascual-Carra, M. A., Rodriguez-Rey, J. C., Fraga, M. F., Bonewald, L., and Riancho, J. A. (2012) DNA methylation contributes to the regulation of sclerostin expression in human osteocytes. *J. Bone Miner. Res* **27,** 926–937
75. Hupkes, M., van Someren, E. P., Middelkamp, S. H., Piek, E., van Zoelen, E. J., and Dechering, K. J. (2011) DNA methylation restricts spontaneous multi-lineage differentiation of mesenchymal progenitor cells, but is stable during growth factor-induced terminal differentiation. *Biochim. Bio-*

phys. Acta **1813,** 839–849
76. Long, F., and Ornitz, D. M. (2013) Development of the endochondral skeleton. *Cold Spring Harb. Perspect. Biol.* **5,**
77. Robbins, D. J., Fei, D. L., and Riobo, N. A. (2012) The hedgehog signal transduction network. *Sci. Signal.* **5,** re6
78. Zhao, M., Qiao, M., Harris, S. E., Chen, D., Oyajobi, B. O., and Mundy, G. R. (2006) The zinc finger transcription factor Gli2 mediates bone morphogenetic protein 2 expression in osteoblasts in response to hedgehog signaling. *Mol. Cell Biol.* **26,** 6197–6208
79. Sinha, S., and Chen, J. K. (2006) Purmorphamine activates the hedgehog pathway by targeting Smoothened. *Nat. Chem. Biol.* **2,** 29–30
80. Wu, X., Ding, S., Ding, Q., Gray, N. S., and Schultz, P. G. (2002) A small molecule with osteogenesis-inducing activity in multipotent mesenchymal progenitor cells. *J Am. Chem. Soc.* **124,** 14520–14521
81. Wu, X., Walker, J., Zhang, J., Ding, S., and Schultz, P. G. (2004) Purmorphamine induces osteogenesis by activation of the hedgehog signaling pathway. *Chem. Biol.* **11,** 1229–1238
82. Chung, U. I., Schipani, E., McMahon, A. P., and Kronenberg, H. M. (2001) Indian hedgehog couples chondrogenesis to osteogenesis in endochondral bone development. *J. Clin. Invest.* **107,** 295–304
83. Long, F., Chung, U. I., Ohba, S., McMahon, J., Kronenberg, H. M., and McMahon, A. P. (2004) Ihh signaling is directly required for the osteoblast lineage in the endochondral skeleton. *Development* **131,** 1309–1318
84. Maeda, Y., Nakamura, E., Nguyen, M. T., Suva, L. J., Swain, F. L., Razzaque, M. S., Mackem, S., and Lanske, B. (2007) Indian hedgehog produced by postnatal chondrocytes is essential for maintaining a growth plate and trabecular bone. *Proc. Natl. Acad. Sci. U.S.A.* **104,** 6382–6387
85. St-Jacques, B., Hammerschmidt, M., and McMahon, A. P. (1999) Indian hedgehog signaling regulates proliferation and differentiation of chondrocytes and is essential for bone formation. *Genes Dev.* **13,** 2072–2086
86. Tian, Y., Xu, Y., Fu, Q., and Dong, Y. (2012) Osterix is required for sonic hedgehog-induced osteoblastic MC3T3-E1 cell differentiation. *Cell Biochem. Biophys.* **64,** 169–176
87. Shimoyama, A., Wada, M., Ikeda, F., Hata, K., Matsubara, T., Nifuji, A., Noda, M., Amano, K., Yamaguchi, A., Nishimura, R., and Yoneda, T. (2007) Ihh/Gli2 signaling promotes osteoblast differentiation by regulating Runx2 expression and function. *Mol. Biol. Cell* **18,** 2411–2418
88. Koziel, L., Wuelling, M., Schneider, S., and Vortkamp, A. (2005) Gli3 acts as a repressor downstream of Ihh in regulating two distinct steps of chondrocyte differentiation. *Development* **132,** 5249–5260
89. Kesper, D. A., Didt-Koziel, L., and Vortkamp, A. (2010) Gli2 activator function in preosteoblasts is sufficient to mediate Ihh-dependent osteoblast differentiation, whereas the repressor function of Gli2 is dispensable for endochondral ossification. *Dev. Dyn.* **239,** 1818–1826
90. Ohba, S., Kawaguchi, H., Kugimiya, F., Ogasawara, T., Kawamura, N., Saito, T., Ikeda, T., Fujii, K., Miyajima, T., Kuramochi, A., Miyashita, T., Oda, H., Nakamura, K., Takato, T., and Chung, U. I. (2008) Patched1 haploinsufficiency increases adult bone mass and modulates Gli3 repressor activity. *Dev. Cell* **14,** 689–699
91. Park, H. L., Bai, C., Platt, K. A., Matise, M. P., Beeghly, A., Hui, C. C., Nakashima, M., and Joyner, A. L. (2000) Mouse Gli1 mutants are viable but have defects in SHH signaling in combination with a Gli2 mutation. *Development* **127,** 1593–1605